AMERICAN SOCIETY FOR MICROBIOLOGY | Microbiology Spectrum

| Bacteriology | Research Article

Growth promotion on maize and whole-genome sequence analysis of *Bacillus velezensis* D103

Yating Zhang,[1,2] Ning Zhang,[1] Xinyue Bi,[2] Tong Bi,[1] Faryal Babar Baloch,[2] Jianjia Miao,[2] Nan Zeng,[2] Bingxue Li,[2] Yingfeng An[1]

AUTHOR AFFILIATIONS See affiliation list on p. 19.

ABSTRACT Root-associated microorganisms, particularly plant growth-promoting rhizobacteria (PGPR) from the *Bacillus* genus, play a crucial role in enhancing crop yield and health. In this study, a *Bacillus* strain was isolated from the rhizosphere soil of maize and identified as *Bacillus velezensis* D103. The primary objective of this research was to evaluate the potential of D103 as a PGPR. Laboratory tests demonstrated that D103 is capable of nitrogen fixation, inorganic phosphorus solubilization, potassium solubilization, and the synthesis of indole-3-acetic acid, ammonia, siderophores, amylase, protease, cellulase, β-1,3-glucanase, and 1-aminocyclopropane-1-carboxylate deaminase. Additionally, D103 exhibited swimming and swarming motility, biofilm formation, and an antagonistic activity against pathogenic fungi. Genome mining identified genes associated with growth promotion and biocontrol activities. In a hydroponics experiment, maize plants treated with a D103 suspension at a cell density of 10^3 CFU·mL^{-1} resulted in the most pronounced showed significant growth stimulation, with shoot length and total root length increasing by 43% and 148%, respectively. These results support the potential of D103 as an effective PGPR for promoting maize crop growth.

IMPORTANCE In this study, we assessed the capacity of D103 to promote plant growth and examined the effects of hydroponic experiments inoculated with this strain on the growth of maize seedlings. We sequenced and analyzed the complete genome of D103, identifying several genes and gene clusters associated with plant growth promotion and resistance to pathogenic fungi, thus revealing the plant growth-promoting mechanisms of this strain. The isolation and characterization of new strains with beneficial traits are essential for expanding microbial resources available for biofertilizer production. Collectively, these findings highlight the promising potential of *Bacillus velezensis* D103 as a biofertilizer for agricultural applications.

KEYWORDS *Bacillus velezensis*, PGPR, genome sequencing, maize, rhizosphere

Modern agricultural practices have significantly enhanced crop yields over the past few decades, primarily through the extensive application of fertilizers and chemical pest control methods (1). However, the reliance on chemical fertilizers and manure to enhance soil fertility and crop productivity has adversely effected complex biogeochemical cycling processes (2). In response to these concerns, scientists and farmers worldwide are adopting organic farming practices, which incorporate traditional agricultural techniques and innovative technologies to replace chemical fertilizers and hazardous pesticides with organic fertilizers and biological control agents (3). Consequently, there is a growing focus on developing novel strategies for organic technologies and exploring their integration with conventional agrochemicals to promote a more sustainable and environmentally friendly agricultural system.

Editor Feng Gao, Tianjin University, Tianjin, China

Address correspondence to Bingxue Li, libingxue@syau.edu.cn, or Yingfeng An, anyingfeng666@163.com.

The authors declare no conflict of interest.

See the funding table on p. 19.

Received 8 May 2024
Accepted 2 September 2024
Published 7 November 2024

Rhizosphere bacteria that facilitate plant growth by providing essential nutrients and regulating plant processes are recognized as plant growth-promoting rhizobacteria (PGPR) (4). PGPR are considered a promising alternative to conventional fertilizer due to their environmentally friendly nature. These beneficial bacteria colonize the root surface or the rhizosphere and enhance plant growth through direct mechanisms such as biological nitrogen fixation (5), mineral solubilization, and production of various phytohormones (6). In addition, PGPR influence plant health through indirect mechanisms, including the production of siderophores (7), 1-aminocyclopropane-1-carboxylate (ACC) deaminase activity (8), volatile organic compound (VOCs) (9), antifungal activity, and induced systemic resistance (ISR) (10). Numerous genera of PGPR have been extensively studied and applied globally to evaluate their plant growth-promoting (PGP) potential, including *Agrobacterium* (8), *Bacillus* (11), *Burkholderia* (12), and *Pseudomonas* (11). These PGPR have demonstrated significant value in sustainable crop production.

Numerous *Bacillus* spp. have been recognized as PGPR and are commercially employed as biofertilizers due to their ability to produce resistant endospores, suppress pathogens, and promote plant growth (13). Among these, *Bacillus amyloliquefaciens*, *Bacillus licheniformis*, and *Bacillus subtilis* are the most extensively utilized species (14). In 1999, *Bacillus velezensis* (CR-502^T) was originally isolated from environmental samples collected from the estuary of the Vélez River, Spain (15). Recently, several strains of *B. velezensis* have gained significant interest for their PGP capabilities, enhancing yield and improving product quality in both greenhouse experiments and field trials (16, 17). *B. velezensis* FZB42 has been formulated into a commercially available inoculant, RhizoVital, to control various soilborne diseases and promote plant growth (18). Genome sequencing strategies have facilitated the investigation of plant growth-promoting genes and secondary metabolite gene clusters in *Bacillus* strains, aiding in the identification of potential PGPR or biocontrol agents (19). Consequently, genetic studies and whole-genome comparisons are highly effective tools for understanding the biological characteristics of PGPR strains.

This study aimed to investigate the PGP properties of *B. velezensis* D103, isolated from the maize rhizosphere. Specifically, the study evaluated (i) potential nutritional contributions, including mineral solubilization and siderophore production; (ii) biochemical and enzymatic functions; (iii) antagonistic effects against fungal pathogens; (iv) genomic analysis and comparative genomics to elucidate the genetic basis of PGP activities and phytopathogen antagonism; and (v) the impact on maize growth.

RESULTS

Identification of strain D103

The morphological examination identified that D103 is a Gram-positive strain capable of spore production. Molecular identification was performed through sequencing of the 16S ribosomal RNA (rRNA) gene (1,547 bp). Basic Local Alignment Search Tool analysis and phylogenetic tree results confirmed that D103 was *Bacillus velezensis* (Fig. 1a). Average nucleotide identity (ANI) results showed that D103 shared more than 98.5% homology with *Bacillus velezensis* GH1-13, *Bacillus amyloliquefaciens* WF02, *Bacillus amyloliquefaciens* MBE1283, *Bacillus velezensis* B1, and *Bacillus amyloliquefaciens* T-5, with *Bacillus velezensis* GH1-13 showing the highest level of similarity (Fig. 1b; Fig. S1).

Characterization with beneficial traits of strain D103

To understand the mechanisms behind the plant growth-promoting effects of strain D103, we evaluated its capacity for nitrogen fixation, inorganic phosphate solubilization, potassium solubilization, and indole-3-acetic acid (IAA) production. Strain D103 demonstrated nitrogen-fixing ability through its growth on nitrogen-free media (Fig. 2a). Nitrogenase activity, measured using the acetylene reduction assay, was 102.49 nmol ethylene·ml^{-1}·h^{-1} (Table 1). Additionally, incubation with Pikovaskaia inorganic phosphate medium and Aleksandrov potassium-solubilizing medium resulted in clear zones

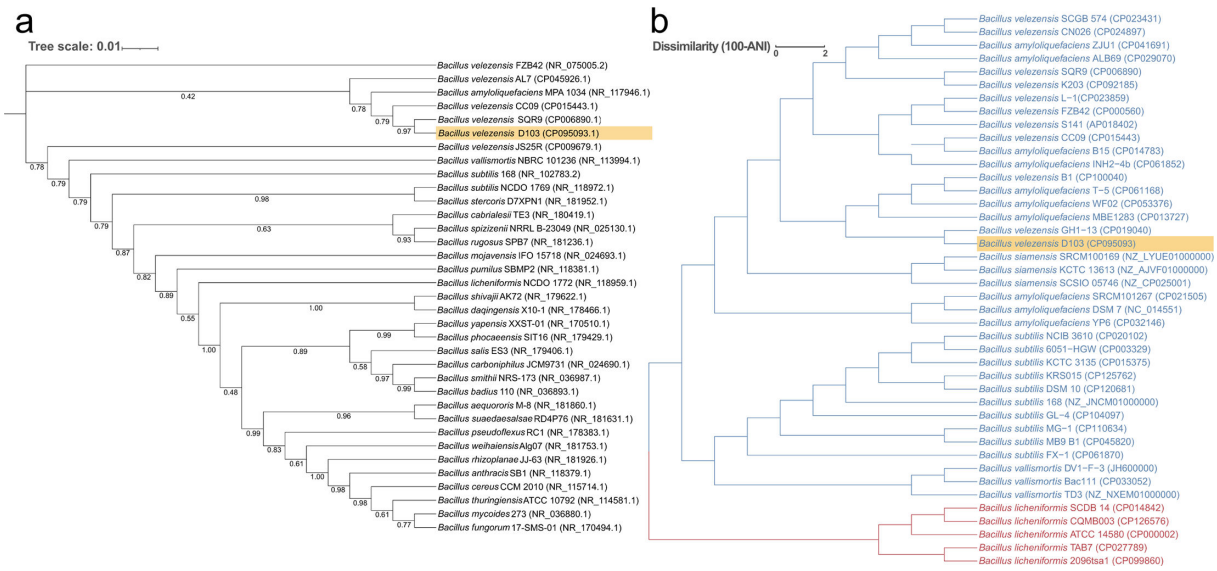

FIG 1 Taxonomic classification of *Bacillus* sp. downloaded from the National Center for Biotechnology Information Reference Sequence Database. (a)Phylogenetic tree depicting the relationships among *Bacillus velezensis* D103 and various other *Bacillus* strains based on 16S rRNA gene sequences. Phylogenetic relationships were determined using a maximum parsimony method, with support values derived from 1,000 replicates. (b)Pairwise average nucleotide identity (ANI) results between 42 *Bacillus* genomes. The similarity among all genomes is represented by a dendrogram using average linkage hierarchical clustering with tree heights corresponding to ANI similarity. Blue branches indicate most of the *Bacillus* genomes, while red branches represent different genomes of *Bacillus licheniformis* sp.

around D103 colonies, indicating its proficiency in solubilizing inorganic phosphorus and potassium (Fig. 2b and c). Quantitative assessments revealed that D103 solubilized inorganic phosphate at a concentration of 68.67 mg·L^{-1} (Table 1). Furthermore, strain D103 produced IAA, as demonstrated by the Salkowski test (Fig. 2e), with ultra-performance liquid chromatography (UPLC) analysis showing a production level of 31.60 mg·L^{-1} (Fig. S2; Table 1).

Strain D103 produces ammonia and siderophores, possesses surface motility, and forms biofilms

Strain D103 produced ammonia, as indicated by the brown coloration of the culture liquid following the addition of Nessler's reagent, confirming a positive result (Fig. 2j). The appearance of a yellow color around D103 colonies on Chrome Azurol S (CAS) agar medium further demonstrated the strain's ability to produce siderophores (Fig. 2d). Motility assessments were conducted on media with varying agar concentrations (0.3% for swimming and 0.7% for swarming). The maximum colony diameter of D103 was observed after 12 h on swimming media and after 18 h on swarming media (Fig. S3). Additionally, strain D103 formed biofilm, as determined by the crystal violet staining method (Table 1). Quantitative analysis of the extracellular polymeric substance (EPS) extracts revealed that the EPS of D103 comprised 58.73 mg·L^{-1} of polysaccharides, 32.05 mg·L^{-1} of proteins, and 8.07 mg·L^{-1} of nucleic acids (Table 1).

In vitro hydrolytic activity of strain D103

In the *in vitro* analysis (Fig. 2f through i; Table 1), strain D103 demonstrated hydrolytic activity, producing cellulase, protease, amylase, β-1,3-glucanase, and ACC deaminase. The enzyme activities measured for D103 were 254.89 U·mL^{-1}, 545.52 U·L^{-1}, 6304.55 U·L^{-1}, 150.83 U·L^{-1} and 32.55 IU·mL^{-1}, respectively.

TABLE 1 Plant growth-promoting factors and hydrolytic enzymes produced by *Bacillus velezensis* D103 at different concentrations

Characteristics	Activity rate
Nitrogenase activity	102.49 ± 3.40 nmol ethylene·ml^{-1}·h^{-1}
Inorganic phosphate solubilization	68.67 ± 4.19 mg·L^{-1}
IAA production	31.60 ± 2.15 mg·L^{-1}
Biofilm production	1.121 ± 0.094
Polysaccharides of EPS[a]	58.73 ± 3.25 mg·L^{-1}
Proteins of EPS	32.05 ± 0.66 mg·L^{-1}
Nucleic acids of EPS	8.07 ± 0.87 mg·L^{-1}
Amylase activity	6304.55 ± 354.78 U·L^{-1}
Cellulase activity	254.89 ± 21.84 U·mL^{-1}
Protease activity	545.52 ± 55.63 U·L^{-1}
ACC deaminase activity	32.55 ± 0.92 IU·mL^{-1}
β−1,3-Glucanase activity	150.83 ± 4.22 U·L^{-1}

[a]EPS, extracellular polymeric substance.

Antagonistic activity against fungal pathogens

In vitro analyses involving five plant pathogenic fungi, demonstrated that strain D103 effectively inhibited the growth of *Fusarium graminearum*, *Athelia rolfsii*, *Fusarium thapsinum*, *Gibberella fujikuroi*, and *Gibberella moniliformis* (Fig. 3).

Genomic characterization of strain D103

The genomic characterization of strain D103 is shown in Fig. 4a, highlighting key features. The genome consists of a circular chromosome measuring 3,857,531 bp, with an average guanine-cytosine (GC) percentage in DNA (GC content) of 46.7%. It contains 3,884 protein-coding genes, 27 rRNA genes, and 86 transfer RNA (tRNA) genes. Functional analysis of the genome sequences was performed using the Cluster of Orthologous Groups of Proteins (COG), Gene Ontology (GO), and Kyoto Encyclopedia of Gene and Genomes (KEGG) databases. The assignments of the genes in these databases are presented in Table 2; Fig. 4.

Among the 3,884 genes present in the D103 genome, 3,239 genes were categorized into 19 categories of the COG database, while 645 genes remained uncategorized (Fig. 4b; Table 2). The largest number of genes was classified into the category of functionally

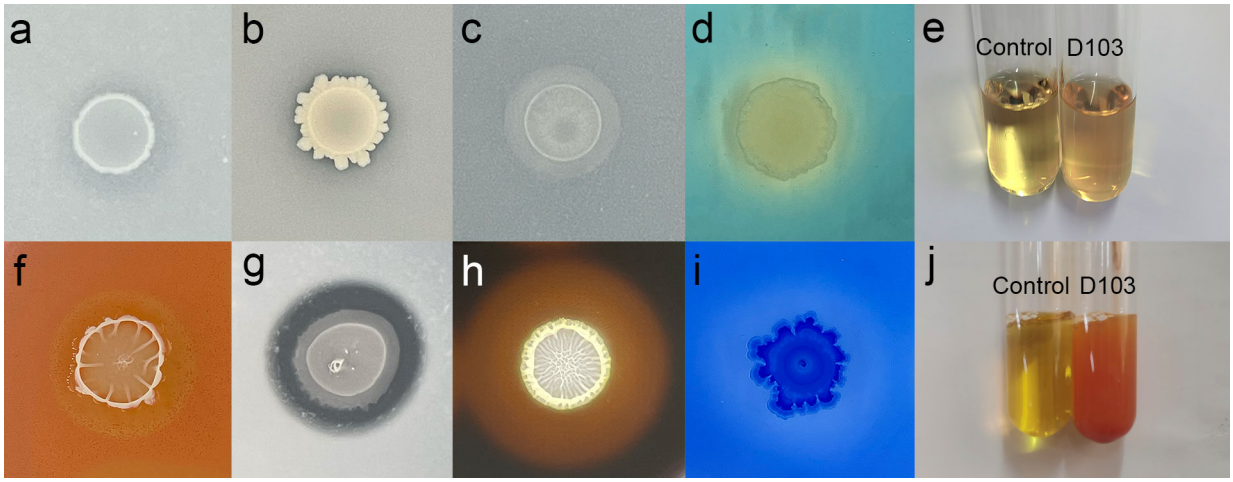

FIG 2 Experimental assessments of plant growth-promoting and hydrolytic enzyme production properties in strain D103. (a) Nitrogen fixation, (b) inorganic phosphorus solubilization, (c) potassium solubilization, (d) siderophore production, (e) IAA production, (f) cellulase production, (g) protease production, (h) amylase production, (i) β-1,3-glucanase production, and (j) ammonia production.

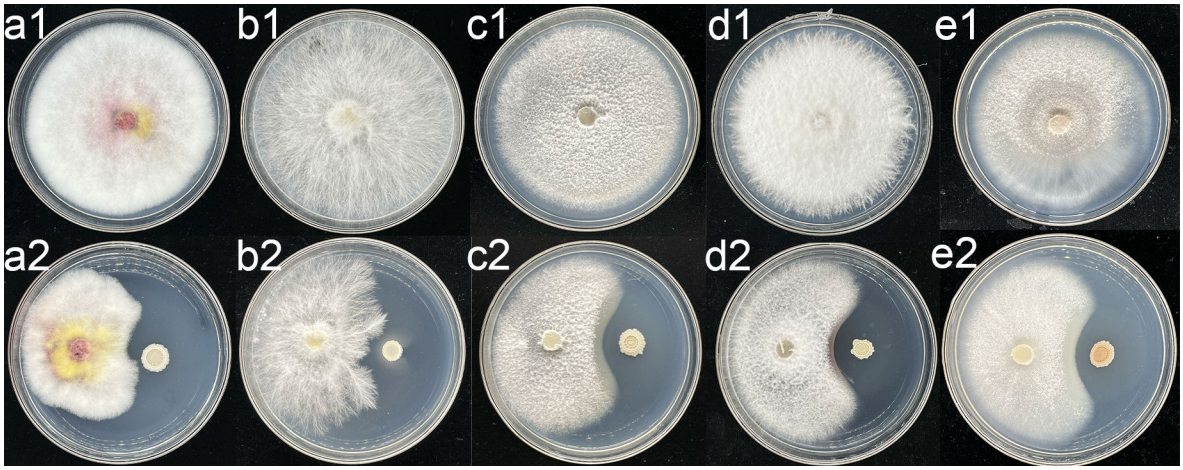

FIG 3 Antifungal activity of strain D103 against various plant pathogenic fungi. (a1 through e1) Placement of a 1-cm agar plug in the center of each potato dextrose agar plate. (a2 through e2) Incubation of strain D103 3.5 cm away from the fungal plugs. Pathogenic fungi included (a) *Fusarium graminearum*, (b) *Athelia rolfsii*, (c) *Fusarium thapsinum*, (d) *Gibberella fujikuroi*, and (e) *Gibberella moniliformis*.

unknown proteins (S), comprising 23.02% with 894 genes. This was followed by amino acid transport and metabolism (E) with 263 genes (6.78%), transcription (K) with 257 genes (6.62%), carbohydrate transport and metabolism (G) with 225 genes (5.79%), cell wall/membrane/envelope biogenesis (M) with 195 genes (5.02%), and energy production and conversion (C) with 179 genes (4.61%).

TABLE 2 Functional categorization of the genome of strain D103 in the COG database

COG categories	Category function	ORF[a] number
A	RNA processing and modification	0
B	Chromatin structure and dynamics	0
C	Energy production and conversion	179
D	Cell cycle control, cell division, and chromosome partitioning	30
E	Amino acid transport and metabolism	263
F	Nucleotide transport and metabolism	79
G	Carbohydrate transport and metabolism	225
H	Coenzyme transport and metabolism	116
I	Lipid transport and metabolism	90
J	Translation, ribosomal structure, and biogenesis	161
K	Transcription	257
L	Replication, recombination, and repair	129
M	Cell wall/membrane/envelope biogenesis	195
N	Cell motility	34
O	Posttranslational modification, protein turnover, and chaperones	94
P	Inorganic ion transport and metabolism	182
Q	Secondary metabolites biosynthesis, transport, and catabolism	86
R	General function prediction only	0
S	Function unknown	894
T	Signal transduction mechanisms	138
U	Intracellular trafficking, secretion, and vesicular transport	31
V	Defense mechanisms	56
W	Extracellular structures	0
Y	Nuclear structure	0
Z	Cytoskeleton	0

[a]ORF, open reading frame.

TABLE 3 Comparative genomic analysis of *B. velezensis* D103, *B. velezensis* FZB42, *B. velezensis* EN01, *B. subtilis* 168, and *B. amyloliquefaciens* X030

General genomic characterization	*B. velezensis* D103	*B. velezensis* FZB42	*B. velezensis* EN01	*B. subtilis* 168	*B. amyloliquefaciens* X030
NCBI accession	CP095093	NC_009725.2	NZ_CP053377.1	NZ_CP010052.1	NZ_CP040672.1
Size (bp)	3,857,531	3,918,596	4,029,600	4,215,619	3,952,640
G + C content (mol%)	46.7	46	46.5	43.5	46.5
Total genes	3,884	3,877	4,002	4,426	3,907
rRNA	27	29	27	30	27
tRNA	86	88	86	86	84
Genomic Island	5	3	17	24	7
Prophage	2	2	6	4	5

The GO database identified 2,678 genes in D103. Among these, 1,364 genes were associated with molecular functions related to binding; 19 genes were associated with cell motility; and 5 genes were associated with locomotion. These functions are associated with the strain's ability to form biofilms and colonize plant tissues (20) (Fig. 4c). Using the KEGG database, we assessed the potential involvement of D103 genes in biological pathways, resulting in the classification of 2,152 genes. The KEGG pathway analysis categorized these genes into 40 functional pathways. The most represented pathways included carbohydrate metabolism (256 genes), amino acid metabolism (371 genes), amino acid metabolism (285 genes), metabolism of cofactors and vitamins (155 genes), membrane transport (140), and signal transduction (139 genes) (Fig. 4d).

Comparative genetic characterization among *Bacillus* spp.

Comparative genomic characterization was conducted among *Bacillus* spp., including reference strains *Bacillus velezensis* FZB42, *Bacillus velezensis* EN01, *Bacillus subtilis* 168, and *Bacillus amyloliquefaciens* X030. Genome sequences were obtained from the National Center for Biotechnology Information (NCBI) database and compared with strain D103, as presented in Table 3. These five strains demonstrated overall similarity in genome size and the number of coding genes. However, differences in the number of genomic islands and prophages were observed, potentially contributing to variations in their genetic profiles. Genomic islands and prophages serve as mobile genetic elements facilitating horizontal gene transfer and play a role in bacterial adaptation and evolution (21).

Core-genome plot analyses of the five *Bacillus* genomes revealed a total of 1,744 genes across these species (Fig. 5a). The distribution showed that 3,135 genes were shared between D103 and *Bacillus subtilis* 168; 2,181 genes were shared between D103 and *Bacillus amyloliquefaciens* X030; and 2,655 genes were shared between D103 and *Bacillus velezensis* EN01. Additionally, 3,353 genes were common between D103 and *Bacillus velezensis* FZB42. D103 shared a considerable number of genes with *B. velezensis* FZB42 and *B. subtilis* 168, suggesting potential similarities with these strains as PGPR. Compared to the other four *Bacillus* strains, D103 contained 358 distinct genes. Among these, 335 genes were associated with assumed proteins and proteins with unknown function, while 21 genes were linked to proteins of known function, including terpene synthase (WP_077722691.1), damage-inducible protein DinB (WP_082998055.1), SAM-dependent methyltransferase (EYB36085.1), NUDIX hydrolase domain-containing protein (AJK64336.1), protein kinase, sporulation protein, and transcriptional regulator, as listed in Table S1.

To assess genetic relationships, whole-genome sequences of the five strains were analyzed using the Mauve program (Fig. 5b). The analysis revealed significant local collinear block (LCB) inversions and gene insertions or deletions in strain D103 relative to *Bacillus amyloliquefaciens* compared to X030 and *Bacillus subtilis* 168. However, D103 showed greater genetic similarity to *Bacillus velezensis* FZB42, with no significant insertions or deletions or LCB inversions observed compared to FZB42 and *Bacillus velezensis* EN01.

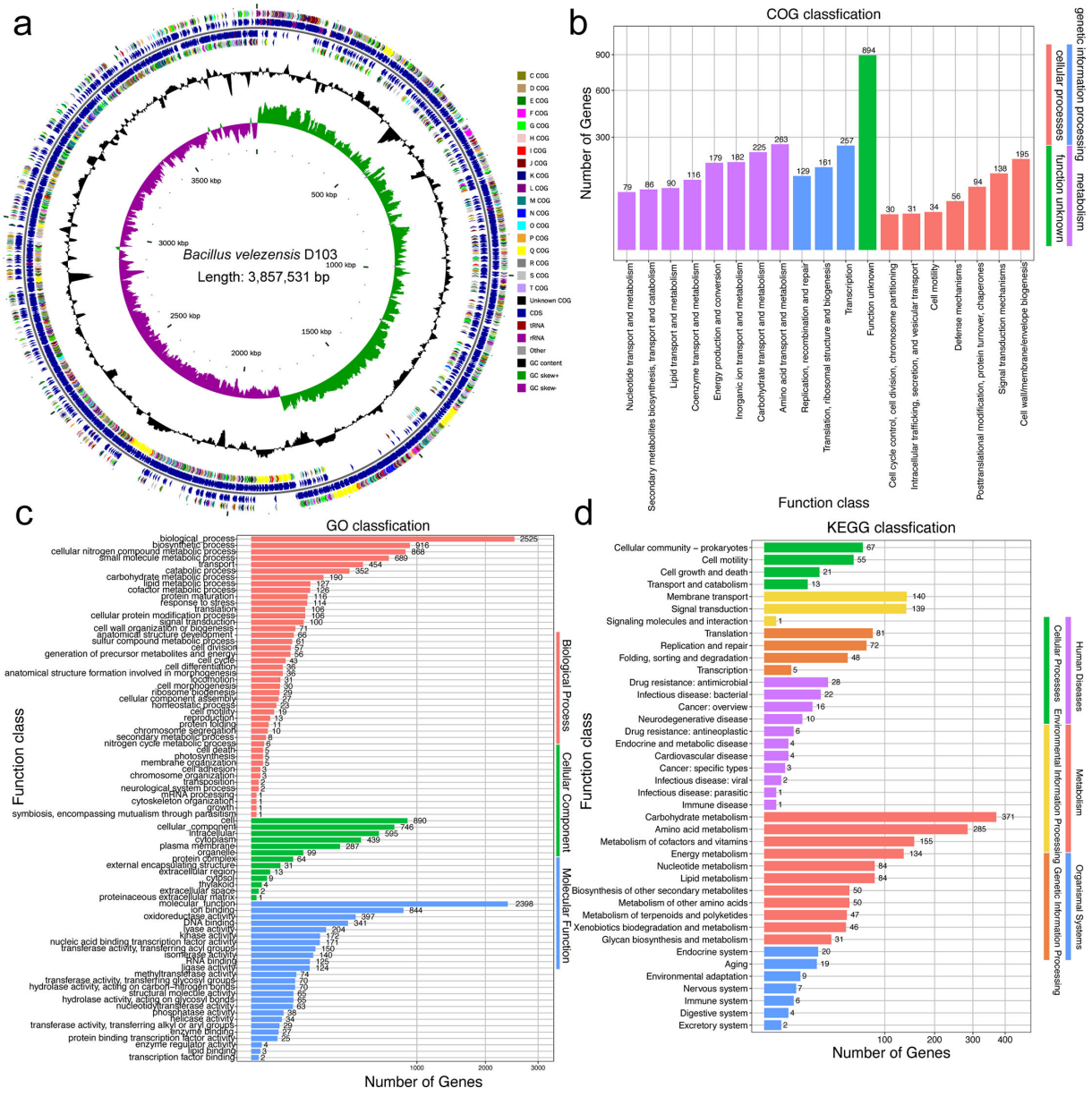

FIG 4 Database annotation for *B. velezensis* D103. (a) A circular genome map is presented, showing the scale; GC skew; GC content; COG classifications for coding DNA sequences (CDS); and the specific positions of CDS, transfer RNA (tRNA), and ribosomal RNA (rRNA) on the genome. This map offers a comprehensive overview of the genomic structure. (b) COG database annotation, (c) GO database annotation, (d) KEGG database annotation.

The annotation analysis of predicted amino acid sequences from strain D103 and four other *Bacillus* strains (FZB42, EN01, 168, and X030) using the dbCAN carbohydrate-active enzyme (CAZyme) database revealed that the D103 genome contains 193 CAZymes. These include 40 glycoside hydrolase (GH) enzymes, 34 glycosyltransferase (GT) enzymes, 17 carbohydrate esterases (CEs), three polysaccharide lyase (PL) enzymes, six auxiliary activities (AAs), and six carbohydrate-binding module (CBM) proteins (Table 4). Enzymes identified in D103, FZB42, EN01, and X030 involve acetylxylan esterase (CE family 6) (EC 3.1.1.72) and monooxygenases (AA family 10), such as lytic xylan monooxygenase/xylan oxidase (glycosidic bond-cleaving) (EC 1.14.99.-), lytic chitin monooxygenase (EC 1.14.99.53), lytic cellulose monooxygenase, lytic cellulose monooxygenase (C1-hydroxylating) (EC 1.14.99.54), and lytic cellulose monooxygenase (C4-dehydrogenating) (EC 1.14.99.56). These enzymes were found in D103, FZB42, EN01, and X030

TABLE 4 Comparative analysis of predicted carbohydrate-active enzyme families in *B. velezensis* D103, *B. velezensis* FZB42, *B. velezensis* EN01, *B. subtilis* 168, and *B. amyloliquefaciens* X030

CAZymes	*B. velezensis* D103	*B. velezensis* FZB42	*B. velezensis* EN01	*B. subtilis* 168	*B. amyloliquefaciens* X030
GH	40	41	42	58	42
GT	34	34	35	39	34
CE	17	17	17	18	17
PL	3	3	3	7	3
AA	6	6	6	5	6
CBM	6	6	6	14	6

but were absent in 168.While the numbers of CAZymes varied among strains, no CAZymes were discovered in D103, indicating similarities in their environmental habitat and nutritional sources. Differences in microbial ability to depolymerize and metabolize sugars may suggest ecological role differentiation to mitigate competition for resources (22).

Genomic analysis of D103 using antiSMASH identified 13 secondary metabolite gene clusters: four NRPS, three TransAT-PKS, two terpenes, one lanthipeptide, and one other KS. These clusters are involved in the biosynthesis of various compounds, including andalusicin A/andalusicin B, surfactin, butirosin A/butirosin B, macrolactin H, bacillaene, fengycin, difficidin, bacillothiazol A-N, bacillibactin, and bacilysin (Table 5). Comparison of the secondary metabolite gene clusters in D103 with those in FZB42, X030, EN01, and 168 (Fig. 6) revealed that five clusters (2, 4–7) were present in each of the *Bacillus* strains. Additionally, four clusters (3, 5, 9, and 10) were shared by D103, FZB42, EN01, and X030; two clusters (12 and 13) were common to D103, FZB42, EN01, and 168; and one cluster (11) was found in both D103 and FZB42. Furthermore, three clusters (4, 8, and 9) were associated with unknown compounds. A distinctive cluster (1) responsible for the production of andalusicin A/andalusicin B was present only in D103.

Plant growth-promoting genes in D103 strain

The D103 genome contains numerous genes predicted to be involved in plant growth-promoting activities (Table S2). Among these, moa clusters (*moaA-E*), responsible for encoding molybdenum cofactors, were identified, suggesting a possible role in nitrogen-fixing gene clusters or cofactors, essential for nitrogen assimilation (23). Additionally, D103 encodes critical elements such as sensor histidine kinase (*glnK*), a gene cluster for nitrate transport and reduction (*nasD-F*), HTH-type transcriptional regulators (*tnrA* and *glnR*), glutamine synthetase (*nifS*), ammonium transporter (*nrgA*), nitrogen regulatory PII-like protein (*nrgB*), a gene cluster for urease subunit (*ureA-C*), a gene cluster for nitrate reductase (*narG-J*), a probable transcription regulator (*arfM*), and nitrite extrusion protein (*narK*). These components contribute to facilitating nitrogen assimilation (24). The genome of D103 revealed the presence of 19 phosphatase genes involved in phosphorus solubilization. Additionally, D103 contained potassium transporter genes, including K^+/H^+ antiporter subunits (*khtS-U*), ktr system potassium uptake proteins (*ktrA*, *ktrC*, and *ktrD*), and putative potassium channel protein (*yugO*) (25). Furthermore, the D103 genome included magnesium transporter genes (*mgtE*, *corA*) (26), manganese assimilation-related genes (*mntH*, *mntR*, and *mntP*) (27), iron assimilation-related genes (*yclQ*, *yusV*, and *yvrA-C*) (28), and a cluster of bivalent cation assimilation-related genes (*tuaA-H*). These genes were hypothesized to play crucial roles in mineral element uptake and the detoxification of heavy metal ions in both bacteria and plants.

PGPR produce VOCs that have the potential to serve as environmentally friendly alternatives to chemical fertilizers. These compounds, including 2,3-butanediol, enhance plant growth by improving nutrient availability, inducing metabolic activities, and stimulating defense responses (29). Analysis of the D103 genome revealed the *als* gene cluster (*alsD*, *alsS*, and *alsR*) and (R,R)-butanediol dehydrogenase (*bdhA*), key components of the biosynthetic pathway for 2,3-butanediol from pyruvate (30). Additionally, we

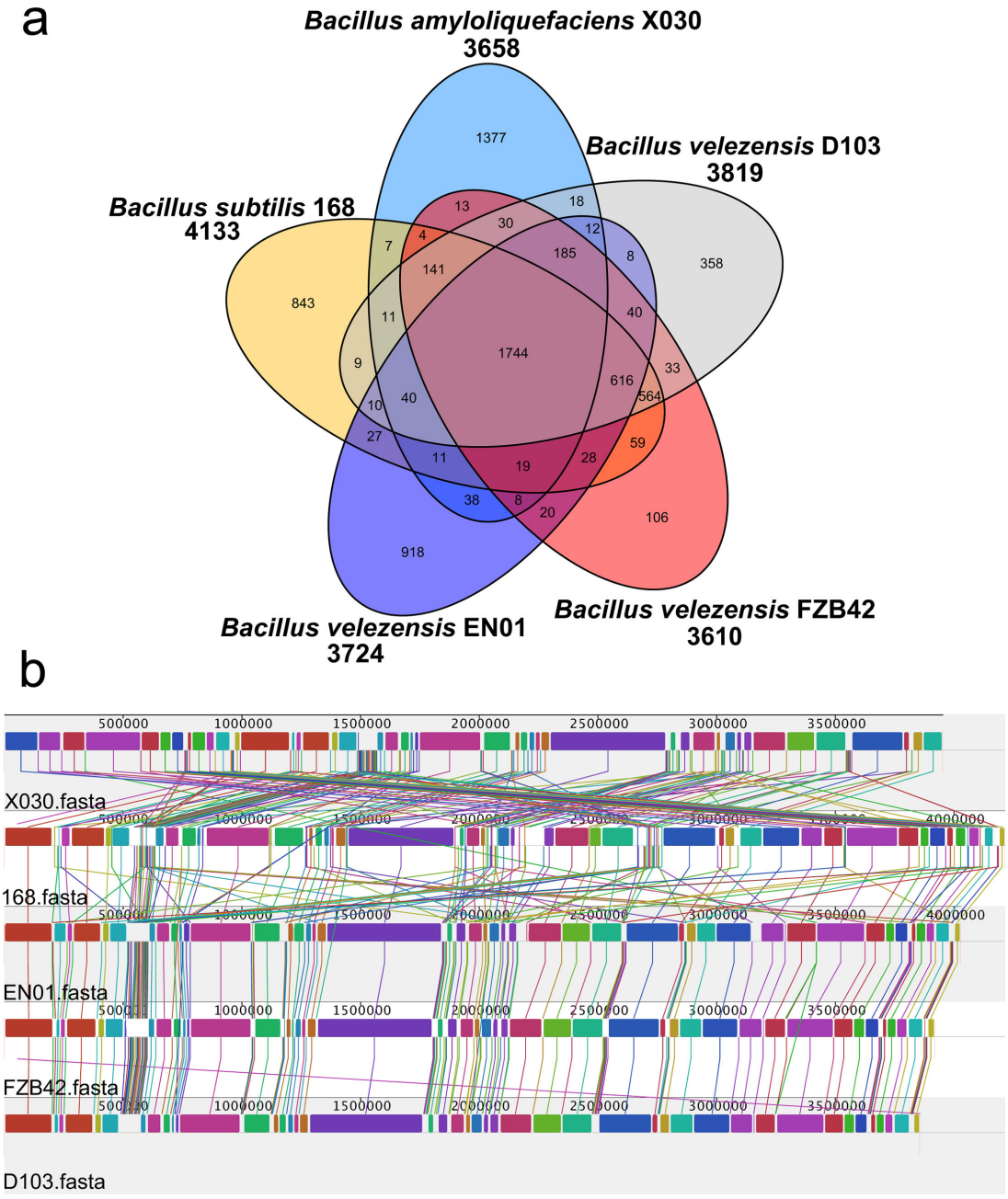

FIG 5 Genomic comparison of *B. velezensis* D103 with *B. velezensis* FZB42, *B. velezensis* EN01, *B. subtilis* 168, and *B. amyloliquefaciens* X030. (a) The Venn diagram illustrates the number of shared and unique clusters of orthologous genes among the strains. (b) Whole-genome comparison using Mauve progressive analysis, highlighting homologous regions, represented by color-coded boxes connected by lines. Forward and reverse regions are differentiated above and below the central axis.

identified the *acu* gene cluster (*acuA-C*) responsible for encoding acetoin, a compound known to promote the development of ISR in plants (31).

The genome of D103 contains genes involved in trehalose biosynthesis (*treP*, *treA*, and *treR*), spermidine and polyamine biosynthesis (*speA*, *speH*, *speB*, *speE*, and *msmX*), and siderophore biosynthesis (*dbhA*, *dbhB*, *dbhC*, *dbhE*, and *dbhF*). These gene clusters contribute to promoting plant growth and inhibiting the growth of plant pathogens (32–34). Additionally, D103 contains 12 genes involved in IAA biosynthesis, utilizing pathways such as indole-3-acetonitrile (*yhcX*, *trpA-F*, *trpP*, and *trpS*) and indole-3-pyruvate (*dhaS*) for IAA synthesis (35). Furthermore, the genome includes genes related

TABLE 5 Comparative analysis of secondary metabolite gene clusters in *Bacillus velezensis* D103 and four other *Bacillus* strains (FZB42, X030, EN01, and 168)

D103		Gene cluster location				Presence (+) or absence (–)			
Cluster number	Type	From	To	Compound	Size (kb)	FZB42	EN01	168	X030
1	Lanthipeptide	193,743	216,358	Andalusicin A/ andalusicin B	22,615	–	–	–	–
2	NRPS	311,522	376,328	Surfactin	64,806	+	+	+	+
3	PKS-like	894,710	935,954	Butirosin A/ butirosin B	41,244	+	+	–	+
4	Terpene	1,020,841	1,037,485	Unknown	16,644	+	+	+	+
5	TransAT-PKS	1,337,888	1,425,686	Macrolactin H	87,798	+	+	–	+
6	TransAT-PKS, T3PKS, NRPS	1,645,193	1,745,891	Bacillaene	100,698	+	+	+	+
7	NRPS, TransAT-PKS, Betalactone	1,812,907	1,947,038	Fengycin	134,131	+	+	+	+
8	Terpene	1,975,295	1,997,178	Unknown	21,883	+	+	+	+
9	T3PKS	2,060,900	2,102,000	Unknown	41,100	+	+	–	+
10	TransAT-PKS	2,229,868	2,323,605	Difficidin	93,737	+	+	–	+
11	NRPS	2,815,113	2,864,622	Bacillothiazol A-N	49,509	+	–	–	–
12	NRPS, RiPP-like	2,965,190	3,016,986	Bacillibactin	51,796	+	+	+	–
13	Other	3,535,967	3,577,385	Bacilysin	41,418	+	+	+	–

to auxin excretion (*ywkB*) and IAA acetylation (*ysnE*), indicating involvement in the tryptophan-independent IAA biosynthetic pathway (19). The presence of phytase genes (*phy*) suggests the potential to degrade phytate, thereby promoting plant growth under phosphate-limited conditions (31).

Effective biofilm production by PGPR enhances their adherence to plant roots and augments plant growth-promoting activities (36). Flagella, motility, and chemotaxis play important roles in all stages of biofilm formation (37). D103 possesses genes associated with bacterial chemotaxis (*che* gene cluster and *mcpA-C*), flagellar assembly (*fli* cluster, *flg* cluster, *flh* cluster, *motAB*), and swarming motility (*swrB-D* and *swrAA*, *efp*). Genes involved in the initial stages of biofilm formation, including histidine kinases (*kinA-D*), master regulators (spo0A, spo0B, spo0E, spo0F, and spo0J), and transcriptional regulators (17 genes), were identified in the genome of D103. Components of the biofilm matrix, including secreted proteins (TasA, TapA, and BslA), mineral scaffolds, extracellular DNA, and extracellular polysaccharides (*eps* gene cluster: *eps*C-O), were also present. Additionally, genes related to biofilm surface formation (*yua*B), colony biofilm strength (*pgs*A), and the development of multicellular communities (*ecs*B, *ylb*F, *ymc*A, and *yqe*K) were identified in the D103 genome (38).

Based on comparative genomic analyses (Table S3), 199 PGP genes were identified in the D103 genome. *Bacillus velezensis* FZB42 and *Bacillus subtilis* 168 shared the most PGP genes with D103, 198 and 195, respectively. Notably, FZB42 was devoid of *sigW*, a gene involved in the transcriptional regulation of biofilm formation, while 168 was devoid of *ybjI*, a gene associated with phosphorus assimilation; *tuaA*, a gene for divalent cation assimilation; *trpC*, a gene for IAA biosynthesis; and swarming motility gene *swrAA*. *Bacillus velezensis* EN01 contains 153 PGP genes shared with D103, whereas *Bacillus amyloliquefaciens* X030 exhibits the lowest number of PGP genes with D103, with only 126 shared genes. Compared to other strains, fewer genes associated with swarming motility, flagellar assembly, and biofilm formation were identified in the genomic comparisons between D103 and both EN01 and X030.

Plant growth-promoting capacity of strain D103

In a hydroponic cultivation system, maize plants were exposed to a range of D103 cell suspension concentration from 10 to 10^6 CFU·mL^{-1}. Growth parameters assessed

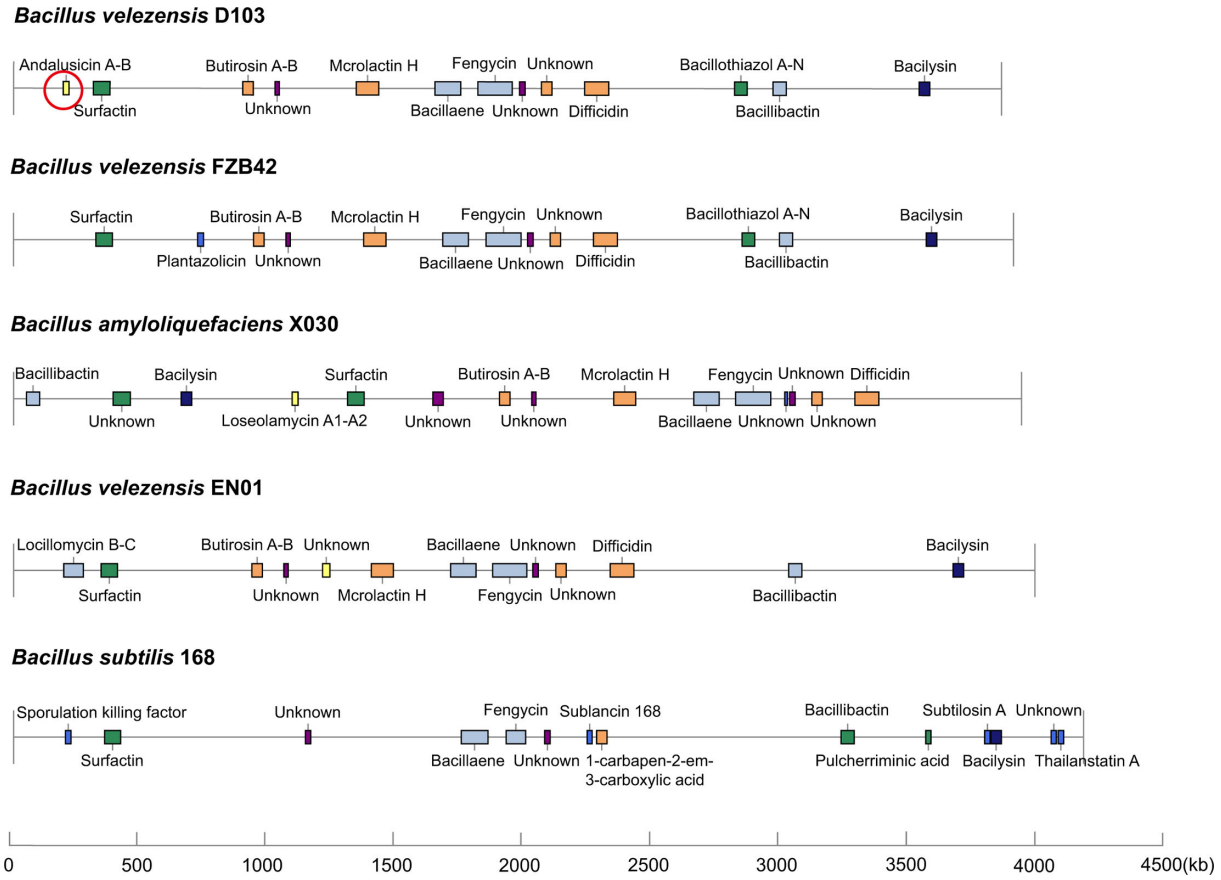

FIG 6 A comparative analysis of the locations of secondary metabolite gene clusters in *B. velezensis* D103, *B. velezensis* FZB42, *B. amyloliquefaciens* X030, *B. velezensis* EN01, and *B. subtilis* 168.

included shoot length (aerial parts), total leaf area, and both fresh and dry weights of the aerial parts. Root development was evaluated based on total root length, surface area, volume, and fresh and dry weight. The results demonstrated a significant impact of D103 cell suspension concentrations on maize plant growth (Fig. 7a; Fig. S4). Specifically, maize seedlings treated with a 10^3 CFU·mL^{-1} D103 cell suspension exhibited significant increases in shoot length and total leaf area, showing 43% and 60% enhancements ($P < 0.001$), respectively, compared to the control group. Additionally, these seedlings demonstrated superiority with total root length reaching 193.62 cm (148% higher than the control), a root surface area of 36.46 cm^2 (114% higher than the control), and a root volume of 0.54 cm^3 (86% higher than the control) (Fig. 7b through e). Moreover, the dry weights of both aerial parts and roots of maize treated with the 10^3 CFU·mL^{-1} D103 cell suspension were significantly increased compared to the control ($P < 0.001$) (Fig. S5). These findings indicate that a D103 cell suspension concentration of 10^3 CFU·mL^{-1} is optimal for enhancing maize plant growth and development.

DISCUSSION

The application of PGPR as biofertilizer represents a viable approach for advancing sustainable agriculture intensification (39). The isolation of *Bacillus* strain D103 from maize rhizosphere soil, combined with phenotypic and phylogenetic analyses, established its classification as *Bacillus velezensis*. This specie is distinguished by its resilience to adverse environmental conditions, secretion of diverse hydrolytic enzymes, enhanced plant growth, exertion of antagonistic effects on phytopathogens, and maintenance of a favorable safety profile, highlighting its significant agricultural potential (40, 41).

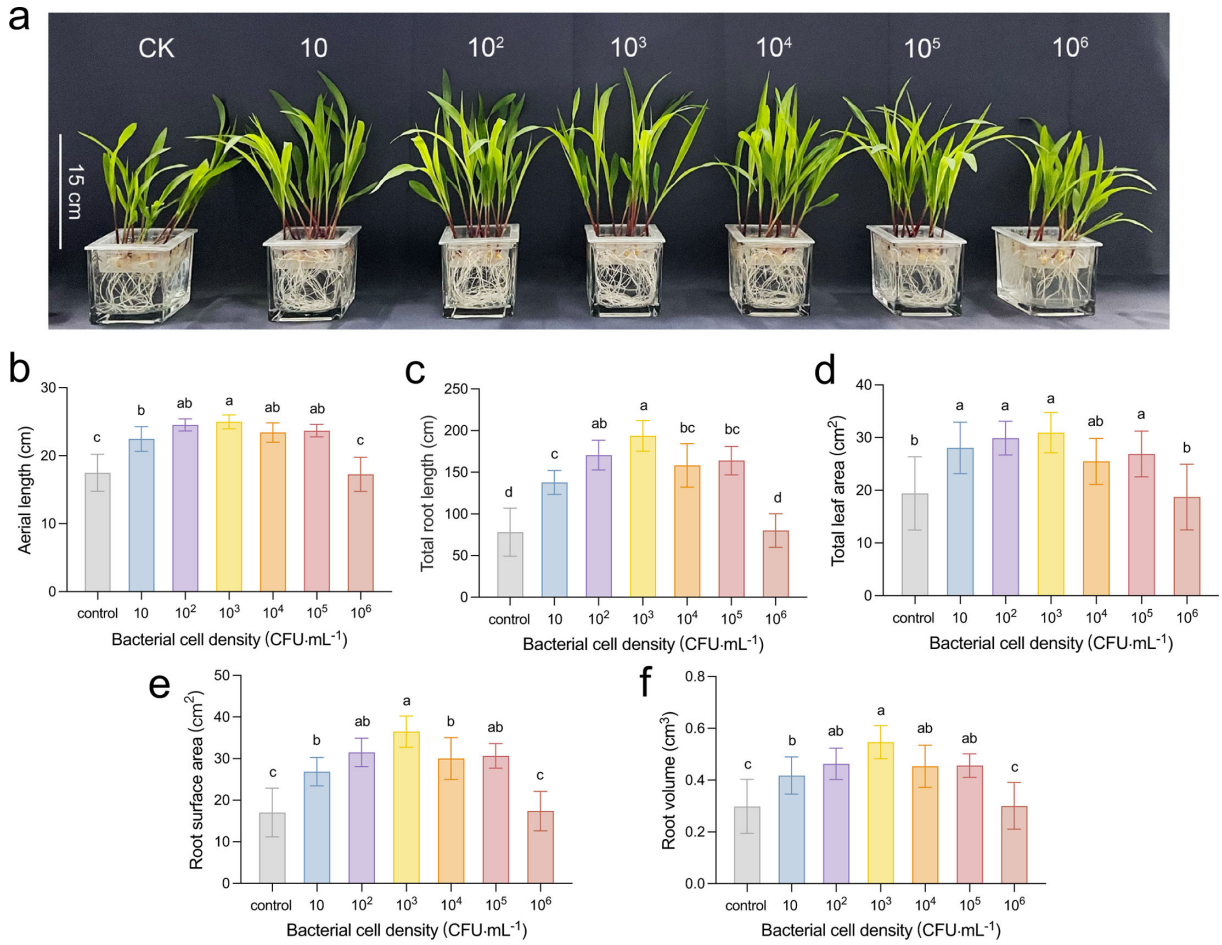

FIG 7 Hydroponic cultivation was employed to assess the growth promotion of maize by applying varying concentrations of the *B. velezensis* D103 strain. (a) Maize growth responses were observed across a range of D103 strain concentrations, from 10 to 10^6 CFU·mL^{-1}, with the control (CK) lacking the D103 strain culture. The agronomic characteristics of maize seedlings were quantified, including (b) aerial length, (c) total root length, (d) total leaf area, (e) root surface area, and (f) root volume. Different letters indicate statistically significant differences between treatments ($P < 0.05$, $n = 10$).

Accordingly, *Bacillus velezensis* D103 demonstrates potential as a PGPR for agricultural applications. This investigation involved a comprehensive characterization of D103 to evaluate its efficacy in promoting plant growth.

Nitrogen is an essential element for plant growth, and nitrogen-fixing bacteria play a crucial role in fixing atmospheric nitrogen into a form that can be utilized by plants, thereby enhancing the soil nitrogen reservoir (5). In this study, *Bacillus velezensis* D103 demonstrated nitrogen-fixing capabilities and thrived in nitrogen-deficient environments. Previous research has established that nitrite reductase, a crucial enzyme nitrogen fixation, is encoded by the *nas* operon. This operon activates transcription by binding to motifs within the TnrA promoter, thereby enhancing the conversion of nitrite, nitrate, and urea into ammonium (42). Twenty-four nitrogen assimilation genes including *nasDEF* and *tnrA* were identified in the D103 genome. Additionally, D103 demonstrated ammonia production, a primary nitrogen source for plants, consequently promoting plant growth. The nitrogen-fixing potential of D103 was demonstrated by acetylene reduction analysis assay.

Phosphorus is a crucial macronutrient for plant growth and development. Due to its rapid immobilization, rendering it inaccessible to plants, phosphate-solubilizing bacteria are essential for converting insoluble phosphorus into bioavailable forms (43). Strain D103 demonstrated the ability to solubilize inorganic phosphorus, thereby enhancing phosphorus availability for plants. Nineteen genes associated with phosphate

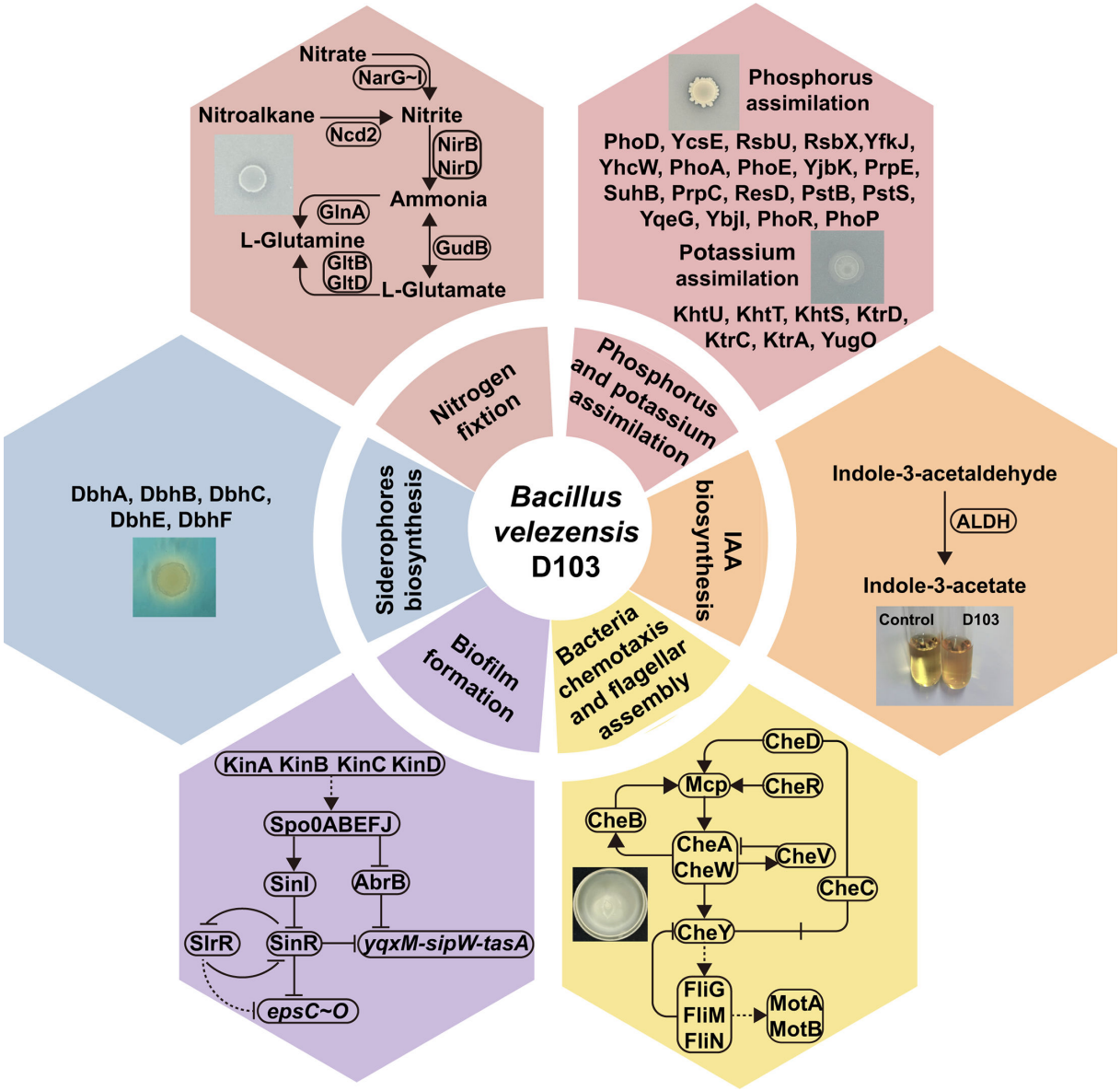

FIG 8 *Bacillus velezensis* D103 possesses beneficial metabolic pathways and genes associated with plant growth-promoting rhizobacteria.

solubilization, including *pstBS* and *phoADEPR*, were identified in strain D103. The *pst*, a phosphate transport system permease, potentially increases phosphate uptake and bioavailability under phosphate-limited conditions (44). Similarly, Torres et al. (45) reported the presence of the organic phosphorus mineralization gene (*phoACDX*) and the P-starvation response regulatory gene (*phoBPR*) in the *Bacillus sensu lato* genome. The phosphorus assimilation gene in D103 increases phosphate utilization in the host plant.

Auxin, particularly IAA, is a critical regulator of plant growth and development, influencing numerous processes, including seedling growth and root formation (46). Previous research has shown that inoculation with IAA-producing *Bacillus amyloliquefaciens* can promote lateral root growth, elongation, and root hair formation in plants such as *Arabidopsis thaliana* (47). This study demonstrated that D103 exhibited IAA production, potentially stimulating root development in the host plant. Notably, plant roots release tryptophan in the rhizosphere, serving as a substrate for IAA biosynthesis by rhizobacteria (48). In this study, 12 genes identified in the D103 genome were putatively

involved in IAA biosynthesis, including *dhaS*, encoding aldehyde dehydrogenase, an enzyme crucial for converting indole-3-acetaldehyde to IAA in the indole-3-pyruvic acid (IPyA) pathway. Studies on *Bacillus amyloliquefaciens* SQR9 have demonstrated that mutation of the *dhaS* gene reduces IAA production to only 23% of wild-type levels (49). These findings suggest that the IPyA pathway is a significant contributor to IAA biosynthesis in D103. Furthermore, D103 possessed genes for synthesizing other potentially beneficial hormones, including trehalose, and phytase. Similar to findings in other bacterial strains, these hormones are implicated in promoting plant growth and enhancing plant tolerance to diverse environmental stresses (50, 51).

Iron, which typically presents in soil as insoluble trivalent Fe^{3+} hydroxide, is not readily assimilated by plants. Siderophores, produced and secreted by bacteria, facilitate the uptake of iron into plant cells (52). The *dhbA-F* operon plays a crucial role in siderophore biosynthesis. Studies have shown that mutants lacking the *ΔdhbA* gene are unable to dehydrogenate (2S,3S)-2,3-dihydroxy-2,3-dihydrobenzoate to 2,3-dihydroxybenzoate (DHB) (53). This inability disrupts extracellular electron transport with ferric iron captured by DHB. This study revealed that D103 possesses the ability to produce siderophores and contains a *dhb* cluster in its genome. Notably, the siderophores produced by D103 contributed to biocontrol by competing for iron, thereby reducing its availability to pathogens (53). The results demonstrated that D103 enhanced Fe^{3+} availability under iron-deficient conditions, which was a key factor promoting maize seedling growth.

Colonization of the plant rhizosphere by bacterial strains is the initial and most crucial step in promoting plant growth and health. Genes associated with motility, chemotaxis, adhesion, and biofilm formation are believed to contribute to colonization (54). While swimming has been identified as the primary mechanism for movement in liquid media, swarming is considered more significant in natural soil environments. In these conditions, dynamic multicellular rafts are formed as groups of cells that move rapidly across solid surfaces, potentially enhancing nutrient acquisition. This phenomenon has been observed in *Bacillus amyloliquefaciens* T-5 colonization nutrient-rich tomato roots (55, 56). The study highlighted the swimming, swarming, and biofilm formation abilities of strain D103, and identified a large number of genes in its genome associated with bacterial chemotaxis, flagellar assembly, swarming motility, and biofilm formation. Bacteria forming biofilms have been reported to exert more beneficial effects on plant growth compared to their planktonic cells counterparts. For instance, *Pseudomonas azotoformans* FAP5 contributes to root colonization and improves wheat performance under stressful conditions (57, 58). Therefore, these characteristics are essential for D103 adaptation, persistence under varying environmental conditions, and the promotion of maize growth.

Biological control of rhizosphere microbes provides host plants natural protection against pathogens (59). The production of secondary metabolites by antagonistic bacteria is the primary mechanism of disease suppression (60). In this study, we identified 13 secondary metabolite gene clusters with antimicrobial activity in the genome of D103. Combined with observed antifungal results, these findings suggested the significant biocontrol potential of D103 as an inoculum. This outcome aligns with previous reports emphasizing the secondary metabolite potential of *B. velezensis* strain (61). Notably, D103 contained a unique cluster of genes responsible for synthesizing andalusicin A and andalusicin B, a novel family of class III lantibiotics derived from *Bacillus thuringiensis* subsp. *andalousiensis* NRRL B23139. This cluster demonstrated biological activity directed at *Bacillus cereus* and related species (62). These findings emphasize the promising potential of D103 for managing plant pathogens in agricultural applications.

Finally, the direct impact of D103 on plant growth was evaluated, revealing a significant enhancement in maize growth when applied at the appropriate concentration. Numerous studies have demonstrated that PGPR stimulate plant root growth and increase root fresh and dry weight, thereby enhancing nutrient uptake (63, 64). D103 increased the length and surface area of corn root structures, offering benefits for

improved ion uptake and nutrient storage. Similarly, other strains of *Bacillus velezensis*, such as SQR9, have been shown to promote cucumber growth through various PGP mechanisms (65). Collectively, these results suggest that D103 has potential as both a maize plant growth promoter and a natural biocontrol agent against plant pathogens.

Conclusion

Bacillus velezensis D103 was evaluated for its plant growth-promoting properties, demonstrating its potential to increase maize plant height and enhance root development. Genomic analyses further validated the findings from *in vitro* assays and hydroponic plant experiments, confirming the efficacy of D103's role as PGPR. The genomic analysis revealed the presence of a multitude of genes potentially involved in plant growth promotion. Collectively, these findings strongly suggest that D103 is a promising candidate for biofertilizer development, with potential application as a single inoculant or as part of a microbial consortium (Fig. 8)

MATERIALS AND METHODS

Isolation and culture conditions of bacteria

Soil samples were collected from the rhizosphere of maize in an experimental field at the Haicheng Branch Campus of Shenyang Agricultural University in Haicheng, China (latitude 40°98′08 N, longitude 122°72′64 E). The field was situated at an elevation of 14.3 m above sea level and had been cultivated with maize crop for >5 years. The area experiences extreme annual temperature variations (−30°C to 34.4°C) and an average annual rainfall of 652 mm. Soil samples were collected in June 2020, and the maize rhizosphere bacterium D103 was isolated using the gradient dilution technique to assess its potential for promoting plant growth. The bacterial strain was cultured in Luria-Bertani (LB) medium, composed of 0.5% yeast extract, 1% sodium chloride, and 1% peptone, with 1.5% agar added for solidification. For long-term preservation, pure cultures were stored at −80°C in an LB medium supplemented with 20% glycerol (vol/vol).

Identification of the strain

Gram staining and spore morphology of the bacterial strain were examined microscopically. The 16S rRNA gene was subjected to colony polymerase chain reaction (PCR) using forward primer 27F (5′-AGAGTTTGATCCTGGCTCAG-3′) and reverse primer 1492R (5′-GGTTACCTTGTTACGACTT-3′) (66). The PCR cycling parameters were as follows: initial denaturation at 94°C for 3 min, followed by 30 cycles of denaturation at 95°C for 40 seconds, annealing at 56°C for 40 seconds, and elongation at 72°C for 90 seconds, with a final extension step at 72°C for 10 min. Purified PCR products were sequenced using an ABI 3730 Genetic Analyzer (Applied Biosystems). The obtained sequences were compared with reference sequences from the NCBI database using Basic Local Alignment Search Tool for Nucleotides software. Reference 16S rRNA sequences were retrieved from GenBank. Sequence alignment was performed using MAFFT (https://mafft.cbrc.jp/alignment/server/). A phylogenetic tree was generated using FastTree (v.2.1.7) (67) with 1,000 bootstrap replicates, and the tree was visualized using ITOL online tool (https://itol.embl.de).

Assessment of *in vitro* plant growth-promoting capacity

To evaluate the nitrogen-fixing capability of strain D103, Ashby's nitrogen-free agar medium was utilized (68). The ability of D103 to grow on this medium indicated its nitrogen-fixing potential. Nitrogenase activity was quantified using the acetylene reduction assay and gas chromatography (GC) as described by Swamy et al. (69). Briefly, strain D103 was inoculated into nitrogen-free Ashby's medium and incubated for 48 h at 37°C with shaking at 180 rpm. Subsequently, 2 mL of the culture was transferred

to 45 mL of Ashby semisolid medium for further incubation. Afterwards, 25 mL of the enriched culture was transferred to 100-mL vials. A sterile syringe replaced 10 mL of air with equivalent acetylene gas and was incubated for 24 h. Nitrogen fixation was assessed by measuring ethylene production using the acetylene reduction assay. The ethylene produced was analyzed using gas chromatography (Shimadzu GC 2010PLUS, Japan) equipped with a flame ionization detector. The chromatographic column used was packed with alumina (3-m length, 0.53-mm diameter). The GC conditions were as follows: oven temperature was maintained at 80°C, while the injector and detector temperatures were set at 165°C. Nitrogen gas and hydrogen gas flow rates were each 40 $mL{\cdot}min^{-1}$, and the air flow rate was 45 $mL{\cdot}min^{-1}$. A 1-mL gas sample was injected, and the peak area for ethylene was measured in relation to a standard ethylene. Ethylene production was expressed as nanoliters of ethylene formed per milliliter of medium per hour at 37°C.

To assess the phosphorus-solubilizing potential of strain D103, modified Pikovaskaia's agar medium was utilized (70). The inoculated plates were incubated at 37°C for 7 days. Phosphorus solubilization was assessed by observing the formation of clear zones around the colonies. The amount of solubilized phosphorus was quantified using the phosphomolybdate method (71).

To assess the potassium-solubilizing capability of strain D103, the Aleksandrov agar medium was used (72). The plates inoculated with the strain, were incubated at 37°C for 7 days. The potassium-solubilizing potential of D103 was determined by observing the formation of clear zones around the colonies, which indicated positive potassium solubilization.

IAA production was assessed using the method described by Mahdi et al. (73), involving the application of Salkowski's reagent. A color change from yellow to pink indicated IAA production. Quantification of IAA was carried out by UPLC following the method described by Shah et al. (74). Briefly, D103 was inoculated into 500 mL of LB medium supplemented with 0.5% L-tryptophan and incubated at 37°C with shaking at 180 rpm for 7 days. The culture liquid phase was centrifuged at 6,500 rpm for 10 min, acidified to pH 2.5–3.0 with 1-N HCl, and extracted with an equal volume of ethyl acetate. The ethyl acetate phase was evaporated under vacuum using a rotary evaporator at 40°C, and the residue was redissolved in 1 mL of methanol and stored at −20°C. UPLC analysis was performed using a Waters H-Class system (Milford, MA, USA) with a C18 column (5 µm, 4.6 × 250 mm). The mobile phase consisted of a water-methanol mixture (60:40) with 0.5% acetic acid, and elution was conducted at a flow rate of 1 $mL{\cdot}min^{-1}$. IAA was detected with a UV-visible detector at 280 nm. Retention times and peak areas were determined using standard IAA calibration curves.

Ammonia and siderophore production, surface motility, and biofilm formation

Bacterial cultures were assessed for ammonia production using Nessler's reagent, as per outlined by Oliva et al. (75). A mixture of 5 mL of supernatant from centrifugation of overnight culture broth with 1 mL of Nessler's reagent indicated NH_3 production by a color change from yellow to brown. Siderophore production was determined using CAS medium (76). Inoculated plates were incubated at 37°C for 4 days, and the presence of an orange-yellow halo around colonies confirmed positive siderophore production.

To assess surface motility, 2.5 µL of each strain cultured overnight (1×10^8 cells) was spotted at the center of LB plates solidified with 0.3% and 0.7% agar. Swimming motility and swarming motility over the surface were analyzed on separate plates (90 mm) (77). Incubation occurred at 37°C for 24 h, with colony diameters measured at 6-h intervals.

Biofilm formation was evaluated in 96-well polystyrene microtiter plates using the crystal violet method (78). $OD_{590\ nm}$ values served as an index of biofilm formation. EPS from strain D103 was extracted using the EDTA extraction method (79). Polysaccharides within the EPS extracts were quantified using a modified phenol-sulfuric acid colorimetric method, employing glucose as the standard (80). Protein content in the EPS extract

was determined using the Coomassie brilliant blue staining method, with bovine serum albumin as the standard (81). Nucleic acids were quantified using the diphenylamine method (82).

Detection of *in vitro* hydrolytic activity

To assess *in vitro* hydrolytic activity, we investigated the production of cellulose (83), protease (84), amylase (85), and β-1,3-glucanase (86) by strain D103, as previously outlined. We quantified the activities of these four enzymes using the Microorganism Cellulase ELISA Kit, Microorganism Protease ELISA Kit, Microorganism Amylase ELISA Kit, and Microorganism β-1,3-glucanase ELISA Kit, all provided by Jiangsu Meimian Industrial Co., Ltd. Additionally, ACC deaminase production and enzyme activity were directly determined using the ACC deaminase ELISA Kit from Jiangsu Meimian Industrial Co., Ltd.

In vitro antagonism assay

To assess the antagonistic effectiveness of D103 against phytopathogens, we selected five fungal pathogens: *Fusarium graminearum*, *Athelia rolfsii*, *Fusarium thapsinum*, *Gibberella fujikuroi*, and *Gibberella moniliformis*. The antifungal resistance of D103 was determined through a triple-replicated dual culture experiment (23). In this experimental setup, strain D103 and each pathogen were simultaneously cultured on 9-cm potato dextrose agar plates, with 8-mm plugs of the pathogen positioned 3.5 cm apart. The plates were then incubated at 28°C for duration of 4 days.

DNA extraction

Genomic DNA extraction was performed using the cetyltrimethylammonium bromide method (87).The DNA was subsequently assessed for concentration, quality, and integrity using a Qubit Fluorometer (Invitrogen, USA) and a Nano Drop Spectrophotometer (Thermo Scientific, USA).

Genome sequencing and assembly

Qualified genomic DNA was fragmented with G-tubes (Covaris, Woburn, MA, USA) and subjected end repair to prepare SMRTbell DNA template libraries with fragment size of>10kb using the blue pippin system, following the manufacturer's specification (PacBio, Menlo Park, CA, USA). The quality of the libraries was assessed using Qubit (v.2.0) Fluorometer (Life Technologies, CA, USA), and the average fragment size was determined with a Bioanalyzer 2100 (Agilent, Santa Clara, CA, USA). SMRT sequencing was performed on the Pacific Biosciences Sequel (PacBio) according to standard protocols.

Qualified genomic DNA was first randomly sonicated, followed by end repair, A-tailing, and adaptor ligation using the NEBNext MLtra DNA Library Prep Kit for Illumina (NEB, USA) in accordance with the manufacturer's protocol. DNA fragments ranging from 300 to 400 bp were selectively enriched by PCR. The PCR products were subsequently purified with the AMPure XP system (Beckman Coulter, Brea, CA, USA). Library size distribution was assessed using a 2100 Bioanalyzer (Agilent), and concentration was determined by real-time PCR. Genome sequencing was performed on the Illumina Novaseq 6000 sequencer utilizing paired-end technology (PE 150).

Continuous long reads obtained from SMRT sequencing were utilized for *de novo* assembly using Falcon (v.0.3.0) (88). Raw data from Illumina platform were processed with FASTP (v.0.20.0) (89) by applying the following standards: (i) reads containing ≥10% unidentified nucleotides (N) were discarded; (ii) reads with ≥50% bases having phred quality scores of ≤20 were excluded; and (iii) reads aligned to the barcode adapter were removed. Following filtration, the resulting clean reads were employed to refine the genome assembly and enhance accuracy. The final genome sequences were determined using Pilon (v.1.23) (90) to correct errors and ensure high-quality assembly.

Genome component prediction

Open reading frames were predicted using the NCBI prokaryotic genome annotation pipeline (91). rRNAs were identified using rRNAmmer (v.1.2) (92), while tRNAs were detected with tRNAscan (v.1.3.1) (93). Small RNAs (sRNAs) were identified with cmscan (v.1.1.2) (94).

Genome composition prediction and annotation

The genome was functionally annotated using several databases, including the Non-redundant Protein Database, GO, KEGG, COG, and Swissprot. To provide a comprehensive overview of the genomic data, CGview (version 2.0.2) (95) was utilized.

Analysis of average nucleotide identity

The ANI of the D103 genome was compared with 41 sequenced *Bacillus* strain genomes FastANI tool (v.1.1) (96). Clustering was performed using bactaxR (v.3.6.1) package in R (97). The phylogenetic tree was generated with ggtree (v.1.16.6) (98), and a heat map was produced using TBtools-II (v.21.0.3) (99). A total of 41 *Bacillus* reference whole-genome sequences were obtained from GenBank for this analysis.

Comparative genomics

In the comparative genomics analysis, four *Bacillus* strains (*Bacillus velezensis* FZB42, *Bacillus velezensis* EN01, *Bacillus subtilis* 168, and *Bacillus amyloliquefaciens* X030) served as reference strains. Genomic characterization utilized NCBI annotated data. Gene families derived from protein sequences of both reference and target bacteria were analyzed using orthoMCL software (v.2.0.8) , resulting in Venn diagrams (100). Genomic comparisons of the five *Bacillus* strains employed Mauve software (v.2.3.1) (101). Genomic islands were identified using the Island Viewer four online platform, while prophages were predicted with the PHASTER online tool (http://phaster.ca/).

Carbohydrate-active enzyme identification

To identify genes encoding CAZymes in the D103 genome, the dbCAN3 database (http://bcb.unl.edu/dbCAN2/) was utilized. This analysis detected various CAZyme categories, including GH, PL, CE, GT, AA, and CBM (102).

Secondary metabolite analysis

To analyze secondary metabolites and identify biosynthetic gene clusters associated with the production of antimicrobial compounds from various chemical classes, the antiSMASH online tool (https://antismash.secondarymetabolites.org) was employed.

Functional gene analysis related to plant growth promotion

The D103 genome was investigated for genes associated with PGP, including those involved in mineral assimilation, IAA synthesis, bacterial chemotaxis, flagellar assembly, and biofilm formation. The sequences identified were compared with the reference sequences in GenBank to validate their accuracy. The PGP-related genes from the D103 genome were compared at the amino acid level with those in the genomes of *Bacillus* strains: FZB42, EN01, 168, and X030 using the NCBI database.

Growth-promoting capacity of D103 on maize

To assess the growth-promoting capabilities of D103 on maize, a bacterial suspension was prepared by incubating D103 for 12 h, resulting in an optical density of $OD_{590\ nm} = 1$ (1×10^8 CFU·mL^{-1}). The suspension was serially diluted with sterile water to achieve final concentrations of 10^6, 10^5, 10^4, 10^3, 10^2, and 10 CFU·mL^{-1}. Maize seeds were sterilized in 75% ethanol for 2 min followed by 1% sodium hypochlorite for 10 min, and subsequently

washed four to five times with sterile water. These seeds were soaked in the different concentrations of bacterial suspensions for 12 h, placed on filter paper in petri dishes with a small amount of distilled water, and allowed to germinate for 3–5 days in the dark at 24°C. Control seeds treated with sterile water were included, and each treatment consisted of three replicates of 10 plants each. Germinated seeds were transferred to the Hoagland hydroponic cultivation system, containing the respective concentrations of the bacterial suspension. The hydroponic solution was replaced every 2 days. All samples were incubated in an artificial climate room mimicking natural maize growing conditions (18°C at night, 24°C during the day, and 65% relative humidity).

After 2 weeks, several parameters were assessed and recorded to evaluate maize seedling growth. These parameters included aerial length, aerial dry weight, and root dry weight. Additional metrics such as root length, root volume, and root surface area were measured using the Root System Analyzer (WinRHIZO, Regent Instruments Inc., Canada). The total leaf area was determined with the Portable Area Meter Model LI-3000C (Li-Cor, Lincoln, NE, USA).

Statistical analysis

Statistical comparisons among treatments were performed using one-way analysis of variance in GraphPad Prism 9 (v.9.5.1). The Shapiro-Wilk test was utilized to evaluate the normality of the data. Results are expressed as the mean ± standard deviation from three independent replicates. Statistical significance was defined as $P < 0.05$.

ACKNOWLEDGMENTS

This work was supported by the National Natural Science Foundation of China (31271818), International Cooperation Project of Universities in Liaoning Province (2023-01), Liaoning Province Rural Science and Technology Special Action Project (2022030673-JH5/104), Shenyang Science and Technology Project (22-319-2-13), Basic Scientific Research Project of Liaoning Provincial Department of Education (JYTYB2024048), and China Scholarship Council (CSC202208850002).

The study was conceived by B.L. and Y.A. Y.Z., T.B., and Y.W. performed the experiments. The data were analyzed by Y.Z., J.M., and N.Z. The manuscript was written mostly by Y.Z. F.B.B., X.B., B.L., and N.Z. revised and edited the text. All authors edited and commented on the final manuscript.

AUTHOR AFFILIATIONS

[1]College of Bioscience and Biotechnology, Shenyang Agricultural University, Shenyang, China
[2]College of Land and Environment, Shenyang Agricultural University, Shenyang, China

AUTHOR ORCIDs

Bingxue Li http://orcid.org/0000-0002-1925-7215
Yingfeng An http://orcid.org/0000-0002-4006-4602

FUNDING

Funder	Grant(s)	Author(s)
MOST | National Natural Science Foundation of China (NSFC)	31271818	Bingxue Li
China Scholarship Council (CSC)	CSC202208850002	Bingxue Li

AUTHOR CONTRIBUTIONS

Yating Zhang, Data curation, Methodology, Visualization, Writing – original draft | Ning Zhang, Validation, Writing – review and editing | Xinyue Bi, Writing – review and editing | Tong Bi, Investigation, Validation | Faryal Babar Baloch, Writing – review and editing | Jianjia Miao, Formal analysis, Software, Visualization | Nan Zeng, Formal analysis | Bingxue Li, Conceptualization, Funding acquisition, Project administration, Resources, Writing – review and editing | Yingfeng An, Conceptualization, Resources, Supervision

DATA AVAILABILITY

The gene sequence of *Bacillus velezensis* D103 is available at the NCBI website with accession number CP095093. The URL of the gene sequence is https://www.ncbi.nlm.nih.gov/nuccore/CP095093.

ADDITIONAL FILES

The following material is available online.

Supplemental Material

Supplemental figures (Spectrum01147-24-S0001.docx). Fig. S1 to S5.
Fig. S6 (Spectrum01147-24-S0002.tif). Mechanism of *Bacillus velezensis* D103 as a PGPR to promote the growth of maize seedlings.
Table S1 (Spectrum01147-24-S0003.xlsx). Unique genes with known functions in *B. velezensis* D103 compared to the other four *Bacillus* strains (FZB42, X030, EN01, and 168).
Table S2 (Spectrum01147-24-S0004.xlsx). Prediction of genes or gene clusters associated with plant growth-promoting activities in the genome of *Bacillus velezensis* D103.
Table S3 (Spectrum01147-24-S0005.xlsx). Comparative analysis of plant growth-promoting genes in D103, FZB42, EN01, 168, and X030.

REFERENCES

1. Ramakrishna W, Yadav R, Li KF. 2019. Plant growth promoting bacteria in agriculture: two sides of a coin. Agric Ecosyst Environ Appl Soil Ecol 138:10–18. https://doi.org/10.1016/j.apsoil.2019.02.019
2. Ray SS, Parihar K, Goyal N, Mahapatra DM. 2024. Synergistic insights into pesticide persistence and microbial dynamics for bioremediation. Environ Res 257:119290. https://doi.org/10.1016/j.envres.2024.119290
3. Wei L, Li J, Qu K, Chen H, Wang M, Xia S, Cai H, Long X-E, Miao Y, Liu D. 2024. Organic fertilizer application promotes the soil nitrogen cycle and plant starch and sucrose metabolism to improve the yield of *Pinellia ternata*. Sci Rep 14:12722. https://doi.org/10.1038/s41598-024-63564-0
4. Li ZB, Song CX, Yi YL, Kuipers OP. 2020. Characterization of plant growth-promoting rhizobacteria from perennial ryegrass and genome mining of novel antimicrobial gene clusters. BMC Genomics 21. https://doi.org/10.1186/s12864-020-6563-7
5. Masood S, Zhao XQ, Shen RF. 2020. *Bacillus pumilus* promotes the growth and nitrogen uptake of tomato plants under nitrogen fertilization. Sci Hortic 272:109581. https://doi.org/10.1016/j.scienta.2020.109581
6. Joshi H, Bisht N, Mishra SK, Prasad V, Chauhan PS. 2023. *Bacillus amyloliquefaciens* modulate carbohydrate metabolism in rice-PGPR cross-talk under abiotic stress and phytohormone treatments. J Plant Growth Regul 42:4466–4483. https://doi.org/10.1007/s00344-023-10913-4
7. Gao BB, Chai XF, Huang YM, Wang XN, Han ZH, Xu XF, Wu T, Zhang XZ, Wang Y. 2022. Siderophore production in *Pseudomonas* SP. strain SP3 enhances iron acquisition in apple rootstock. J Appl Microbiol 133:720–732. https://doi.org/10.1111/jam.15591
8. Zafar-ul-Hye M, Danish S, Abbas M, Ahmad M, Munir TM. 2019. ACC deaminase producing PGPR *Bacillus amyloliquefaciens* and agrobacterium fabrum along with biochar improve wheat productivity under drought stress. Agronomy-Basel 9:343. https://doi.org/10.3390/agronomy9070343
9. Mhlongo MI, Piater LA, Dubery IA. 2022. Profiling of volatile organic compounds from four plant growth-promoting rhizobacteria by SPME–GC–MS: a metabolomics study. Metabolites 12:763. https://doi.org/10.3390/metabo12080763
10. Li ZJ, Tang SY, Gao HS, Ren JY, Xu PL, Dong WP, Zheng Y, Yang W, Yu YY, Guo JH, Luo YM, Niu DD, Jiang CH. 2024. Plant growth-promoting rhizobacterium *Bacillus cereus* AR156 induced systemic resistance against multiple pathogens by priming of camalexin synthesis. Plant Cell Environ 47:337–353. https://doi.org/10.1111/pce.14729
11. Comeau D, Balthazar C, Novinscak A, Bouhamdani N, Joly DL, Filion M. 2021. Interactions between *Bacillus* Spp., *Pseudomonas* Spp. and *Cannabis sativa* promote plant growth. Front Microbiol 12. https://doi.org/10.3389/fmicb.2021.715758
12. Xu Y, Li Y, Long CM, Han LZ. 2022. Alleviation of salt stress and promotion of growth in peanut by *Tsukamurella tyrosinosolvens* and *Burkholderia pyrrocinia*. Biologia 77:2423–2433. https://doi.org/10.1007/s11756-022-01073-z
13. Dame ZT, Rahman M, Islam T. 2021. *Bacilli* as sources of agrobiotechnology: recent advances and future directions. Green Chem Lett Rev 14:246–271. https://doi.org/10.1080/17518253.2021.1905080
14. Adeniji AA, Loots DT, Babalola OO. 2019. *Bacillus velezensis*: phylogeny, useful applications, and avenues for exploitation. Appl Microbiol Biotechnol 103:3669–3682. https://doi.org/10.1007/s00253-019-09710-5
15. Ruiz-García C, Béjar V, Martínez-Checa F, Llamas I, Quesada E. 2005. *Bacillus velezensis* sp. nov., a surfactant-producing bacterium isolated from the river Vélez in Málaga, southern Spain. Int J Syst Evol Microbiol 55:191–195. https://doi.org/10.1099/ijs.0.63310-0

16. Hong S, Kim TY, Won SJ, Moon JH, Ajuna HB, Kim KY, Ahn YS. 2022. Control of fungal diseases and fruit yield improvement of strawberry using *Bacillus velezensis* CE 100. Microorganisms 10:365. https://doi.org/10.3390/microorganisms10020365
17. Joly P, Calteau A, Wauquier A, Dumas R, Beuvin M, Vallenet D, Crovadore J, Cochard B, Lefort F, Berthon JY. 2021. From strain characterization to field authorization: highlights on *Bacillus velezensis* strain B25 beneficial properties for plants and its activities on phytopathogenic fungi. Microorganisms 9:1924. https://doi.org/10.3390/microorganisms9091924
18. Rabbee MF, Ali MS, Choi J, Hwang BS, Jeong SC, Baek KH. 2019. *Bacillus velezensis:* a valuable member of bioactive molecules within plant microbiomes. Molecules 24:1046. https://doi.org/10.3390/molecules24061046
19. Balderas-Ruíz KA, Bustos P, Santamaria RI, González V, Cristiano-Fajardo SA, Barrera-Ortíz S, Mezo-Villalobos M, Aranda-Ocampo S, Guevara-García ÁA, Galindo E, Serrano-Carreón L. 2020. *Bacillus velezensis* 83 a bacterial strain from mango phyllosphere, useful for biological control and plant growth promotion. AMB Express 10:163. https://doi.org/10.1186/s13568-020-01101-8
20. Rashmi BS, Gayathri D. 2017. Draft genome sequence of the gluten-hydrolyzing bacterium *Bacillus subtilis* GS 188, isolated from wheat sourdough. Genome Announc 5:e00952-17. https://doi.org/10.1128/genomeA.00952-17
21. Huang JH, Dai XY, Wu ZW, Hu X, Sun JJ, Tang YJ, Zhang WQ, Han PZ, Zhao JQ, Liu GJ, Wang XM, Mao SY, Wang Y, Call DR, Liu JX, Wang LP. 2023. Conjugative transfer of *Streptococcal* prophages harboring antibiotic resistance and virulence genes. ISME J 17:1467–1481. https://doi.org/10.1038/s41396-023-01463-4
22. Pallister E, Gray CJ, Flitsch SL. 2020. Enzyme promiscuity of carbohydrate active enzymes and their applications in biocatalysis. Curr Opin Struct Biol 65:184–192. https://doi.org/10.1016/j.sbi.2020.07.004
23. Kamali M, Guo DJ, Naeimi S, Ahmadi J. 2022. Perception of biocontrol potential of *Bacillus inaquosorum* KR2-7 against *Tomato fusarium* wilt through merging genome mining with chemical analysis. Biology (Basel) 11:137. https://doi.org/10.3390/biology11010137
24. Zhou XQ, Wang YL, Tan X, Sheng YQ, Li YB, Zhang Q, Xu JL, Shi ZS. 2023. Genomics and nitrogen metabolic characteristics of a novel heterotrophic nitrifying-aerobic denitrifying bacterium *Acinetobacter oleivorans* AHP123. Bioresour Technol 375:128822. https://doi.org/10.1016/j.biortech.2023.128822
25. Cereija TB, Guerra JPL, Jorge JMP, Morais-Cabral JH. 2021. C-di-AMP, a likely master regulator of bacterial K+ homeostasis machinery, activates a K+ exporter. Proc Natl Acad Sci USA 118:e2020653118. https://doi.org/10.1073/pnas.2020653118
26. Franken GAC, Huynen MA, Martínez-Cruz LA, Bindels RJM, de Baaij JHF. 2022. Structural and functional comparison of magnesium transporters throughout evolution. Cell Mol Life Sci 79:418. https://doi.org/10.1007/s00018-022-04442-8
27. Ouyang A, Gasner KM, Neville SL, McDevitt CA, Frawley ER. 2022. MntP and YiiP contribute to manganese efflux in *Salmonella enterica* serovar *Typhimurium* under conditions of manganese overload and nitrosative stress. Microbiol Spectr 10:e0131621. https://doi.org/10.1128/spectrum.01316-21
28. Hastie JL, Carmichael HL, Werner BM, Dunbar KE, Carlson PE Jr. 2023. *Clostridioides difficile* utilizes siderophores as an iron source and FhuDBGC contributes to ferrichrome uptake. J Bacteriol 205:e0032423. https://doi.org/10.1128/jb.00324-23
29. Netzker T, Shepherdson EMF, Zambri MP, Elliot MA. 2020. Bacterial volatile compounds: functions in communication, cooperation, and competition. Annu Rev Microbiol 74:409–430. https://doi.org/10.1146/annurev-micro-011320-015542
30. Li YC, Zhao XY, Yao MJ, Yang WL, Han YL, Liu LP, Zhang JX, Liu JJ. 2023. Mechanism of microbial production of acetoin and 2,3-butanediol optical isomers and substrate specificity of butanediol dehydrogenase. Microb Cell Fact 22. https://doi.org/10.1186/s12934-023-02163-6
31. Zhang N, Yang DQ, Wang DD, Miao YZ, Shao JH, Zhou X, Xu ZH, Li Q, Feng HC, Li SQ, Shen QR, Zhang RF. 2015. Whole transcriptomic analysis of the plant-beneficial rhizobacterium *Bacillus amyloliquefaciens* SQR9 during enhanced biofilm formation regulated by maize root exudates. BMC Genomics 16:685. https://doi.org/10.1186/s12864-015-1825-5
32. Ahmad HM, Fiaz S, Hafeez S, Zahra S, Shah AN, Gul B, Aziz O, Mahmood-Ur-Rahman A, Fakhar A, Rafique M, Chen YL, Yang SH, Wang XK. 2022. Plant growth-promoting rhizobacteria eliminate the effect of drought stress in plants: a review. Front Plant Sci 13:875774. https://doi.org/10.3389/fpls.2022.875774
33. Gowtham HG, Singh SB, Shilpa N, Aiyaz M, Nataraj K, Udayashankar AC, Amruthesh KN, Murali M, Poczai P, Gafur A, Almalki WH, Sayyed RZ. 2022. Insight into recent progress and perspectives in improvement of antioxidant machinery upon PGPR augmentation in plants under drought stress: a review. Antioxidants (Basel) 11:1763. https://doi.org/10.3390/antiox11091763
34. Fahde S, Boughribil S, Sijilmassi B, Amri A. 2023. Rhizobia: a promising source of plant growth-promoting molecules and their non-legume interactions: examining applications and mechanisms. Agriculture-Basel13:1279. https://doi.org/10.3390/agriculture13071279
35. Yin ZQ, Wang X, Hu YJ, Zhang JK, Li H, Cui YR, Zhao DY, Dong XS, Zhang XH, Liu K, Du BH, Ding YQ, Wang CQ. 2022. *Metabacillus dongyingensis* sp is represented by the plant growth-promoting bacterium BY2G20 isolated from saline-alkaline soil and enhances the growth of *Zea mays* L. under salt stress. mSystems 7. https://doi.org/10.1128/msystems.01426-21
36. Santoyo G, Urtis-Flores CA, Loeza-Lara PD, Orozco-Mosqueda MDC, Glick BR. 2021. Rhizosphere colonization determinants by plant growth-promoting rhizobacteria (PGPR). Biology (Basel) 10:475. https://doi.org/10.3390/biology10060475
37. Colin R, Ni B, Laganenka L, Sourjik V. 2021. Multiple functions of flagellar motility and chemotaxis in bacterial physiology. FEMS Microbiol Rev 45:fuab038. https://doi.org/10.1093/femsre/fuab038
38. Arnaouteli S, Bamford NC, Stanley-Wall NR, Kovács ÁT. 2021. *Bacillus subtilis* biofilm formation and social interactions. Nat Rev Microbiol 19:600–614. https://doi.org/10.1038/s41579-021-00540-9
39. Basu A, Prasad P, Das SN, Kalam S, Sayyed RZ, Reddy MS, El Enshasy H. 2021. Plant growth promoting rhizobacteria (PGPR) as green bioinoculants: recent developments, constraints, and prospects. Sustainability 13:1140. https://doi.org/10.3390/su13031140
40. Khalid F, Khalid A, Fu YC, Hu Q, Zheng YF, Khan S, Wang ZG. 2021. Potential of *Bacillus velezensis* as a probiotic in animal feed: a review. J Microbiol 59:627–633. https://doi.org/10.1007/s12275-021-1161-1
41. Arsov A, Petrov K, Petrova P. 2021. Enhanced activity by genetic complementarity: heterologous secretion of clostridial cellulases by *Bacillus licheniformis* and *Bacillus velezensis* Molecules 26:5625. https://doi.org/10.3390/molecules26185625
42. He HH, Li YR, Zhang L, Ding ZY, Shi GY. 2023. Understanding and application of *Bacillus* nitrogen regulation: a synthetic biology perspective. J Adv Res 49:1–14. https://doi.org/10.1016/j.jare.2022.09.003
43. Mažylytė R, Kaziūnienė J, Orola L, Valkovska V, Lastauskienė E, Gegeckas A. 2022. Phosphate solubilizing microorganism *Bacillus* sp. MVY-004 and its significance for biomineral fertilizers' development in agrobiotechnology. Biology (Basel) 11:254. https://doi.org/10.3390/biology11020254
44. Adeleke BS, Ayangbenro AS, Babalola OO. 2021. Genomic analysis of endophytic *Bacillus cereus* T4S and its plant growth-promoting traits. Plants (Basel) 10:1776. https://doi.org/10.3390/plants10091776
45. Torres P, Altier N, Beyhaut E, Fresia P, Garaycochea S, Abreo E. 2024. Phenotypic, genomic and in planta characterization of *Bacillus sensu lato* for their phosphorus biofertilization and plant growth promotion features in soybean. Microbiol Res 280:127566. https://doi.org/10.1016/j.micres.2023.127566
46. Nguyen LTT, Park AR, Van Le V, Hwang I, Kim J-C. 2024. Exploration of a multifunctional biocontrol agent *Streptomyces* sp. JCK-8055 for the management of apple fire blight. Appl Microbiol Biotechnol 108:21–21. https://doi.org/10.1007/s00253-023-12874-w
47. Asari S, Tarkowská D, Rolčík J, Novák O, Palmero DV, Bejai S, Meijer J. 2017. Analysis of plant growth-promoting properties of *Bacillus amyloliquefaciens* UCMB5113 using *Arabidopsis thaliana* as host plant. Planta 245:15–30. https://doi.org/10.1007/s00425-016-2580-9
48. Shameer S, Prasad T. 2018. Plant growth promoting rhizobacteria for sustainable agricultural practices with special reference to biotic and abiotic stresses. Plant Growth Regul 84:603–615. https://doi.org/10.1007/s10725-017-0365-1

49. Shao JH, Li YC, Li ZF, Xu ZH, Xun WB, Zhang N, Feng HC, Miao YZ, Shen QR, Zhang RF. 2021. Participating mechanism of a major contributing gene *ysnE* for auxin biosynthesis in *Bacillus amyloliquefaciens* SQR9 . J Basic Microbiol 61:569–575. https://doi.org/10.1002/jobm.202100098
50. Onwe RO, Onwosi CO, Ezugworie FN, Ekwealor CC, Okonkwo CC. 2022. Microbial trehalose boosts the ecological fitness of biocontrol agents, the viability of probiotics during long-term storage and plants tolerance to environmental-driven abiotic stress. Sci Total Environ 806:150432. https://doi.org/10.1016/j.scitotenv.2021.150432
51. Idriss EE, Makarewicz O, Farouk A, Rosner K, Greiner R, Bochow H, Richter T, Borriss R. 2002. Extracellular phytase activity of *Bacillus amyloliquefaciens* FZB45 contributes to its plant-growth-promoting effect. Microbiol (Reading, Engl):2097–2109. https://doi.org/10.1099/00221287-148-7-2097
52. Vocciante M, Grifoni M, Fusini D, Petruzzelli G, Franchi E. 2022. The role of plant growth-promoting rhizobacteria (PGPR) in mitigating plant's environmental stresses. Appl Sci (Basel) 12:1231. https://doi.org/10.3390/app12031231
53. Andrić S, Rigolet A, Argüelles Arias A, Steels S, Hoff G, Balleux G, Ongena L, Höfte M, Meyer T, Ongena M. 2023. Plant-associated *Bacillus* mobilizes its secondary metabolites upon perception of the siderophore pyochelin produced by a *Pseudomonas* competitor . ISME J 17:263–275. https://doi.org/10.1038/s41396-022-01337-1
54. Zhao Y, Ding WJ, Xu L, Sun JQ. 2024. A comprehensive comparative genomic analysis revealed that plant growth promoting traits are ubiquitous in strains of *Stenotrophomonas*. Front Microbiol 15. https://doi.org/10.3389/fmicb.2024.1395477
55. Blake C, Christensen MN, Kovács ÁT. 2021. Molecular aspects of plant growth promotion and protection by *Bacillus subtilis* Mol Plant Microbe Interact 34:15–25. https://doi.org/10.1094/MPMI-08-20-0225-CR
56. Tan SY, Yang CL, Mei XL, Shen SY, Raza W, Shen QR, Xu YC. 2013. The effect of organic acids from tomato root exudates on rhizosphere colonization of *Bacillus amyloliquefaciens* T-5.Appl Soil Ecol 64:15–22. https://doi.org/10.1016/j.apsoil.2012.10.011
57. Ajijah N, Fiodor A, Pandey AK, Rana A, Pranaw K. 2023. Plant growth-promoting bacteria (PGPB) with biofilm-forming ability: a multifaceted agent for sustainable agriculture. Diversity (Basel) 15:112. https://doi.org/10.3390/d15010112
58. Ansari FA, Jabeen M, Ahmad I. 2021. *Pseudomonas azotoformans* FAP5, a novel biofilm-forming PGPR strain, alleviates drought stress in wheat plant. Int J Environ Sci Technol 18:3855–3870. https://doi.org/10.1007/s13762-020-03045-9
59. Pandit MA, Kumar J, Gulati S, Bhandari N, Mehta P, Katyal R, Rawat CD, Mishra V, Kaur J. 2022. Major biological control strategies for plant pathogens. Pathogens 11:273. https://doi.org/10.3390/pathogens11020273
60. Khatri S, Sazinas P, Strube ML, Ding L, Dubey S, Shivay YS, Sharma S, Jelsbak L. 2023. *Pseudomonas* is a key player in conferring disease suppressiveness in organic farming. Plant Soil. https://doi.org/10.1007/s11104-023-05927-6
61. Sam-On MFS, Mustafa S, Mohd Hashim A, Yusof MT, Zulkifly S, Malek AZA, Roslan MAH, Mohd Asrore MS. 2023. Mining the genome of *Bacillus velezensis* FS26 for probiotic markers and secondary metabolites with antimicrobial properties against aquaculture pathogens. Microb Pathog 181:106161. https://doi.org/10.1016/j.micpath.2023.106161
62. Grigoreva A, Andreeva J, Bikmetov D, Rusanova A, Serebryakova M, Garcia AH, Slonova D, Nair SK, Lippens G, Severinov K, Dubiley S. 2021. Identification and characterization of andalusicin: N-terminally dimethylated class III lantibiotic from *Bacillus thuringiensis sv. andalousiensis*. Iscience 24:102480. https://doi.org/10.1016/j.isci.2021.102480
63. Farhaoui A, Adadi A, Tahiri A, El Alami N, Khayi S, Mentag R, Ezrari S, Radouane N, Mokrini F, Belabess Z, Lahlali R. 2022. Biocontrol potential of plant growth-promoting rhizobacteria (PGPR) against *Sclerotiorum rolfsii* diseases on sugar beet (*Beta vulgaris* L.). Physiol Mol Plant Pathol 119:101829. https://doi.org/10.1016/j.pmpp.2022.101829
64. Ejaz S, Batool S, Anjum MA, Naz S, Qayyum MF, Naqqash T, Shah KH, Ali S. 2020. Effects of inoculation of root-associative *Azospirillum* and *Agrobacterium* strains on growth, yield and quality of pea (*Pisum sativum* L.) grown under different nitrogen and phosphorus regimes. Sci Hortic 270:109401. https://doi.org/10.1016/j.scienta.2020.109401
65. Huang R, Feng HC, Xu ZH, Zhang N, Liu YP, Shao JH, Shen QR, Zhang RF. 2022. Identification of adhesins in plant beneficial rhizobacteria *Bacillus velezensis* SQR9 and their effect on root colonization. Mol Plant Microbe Interact 35:64–72. https://doi.org/10.1094/MPMI-09-21-0234-R
66. Miyoshi T, Iwatsuki T, Naganuma T. 2005. Phylogenetic characterization of 16S rRNA gene clones from deep-groundwater microorganisms that pass through 0.2-micrometer-pore-size filters. Appl Environ Microbiol 71:1084–1088. https://doi.org/10.1128/AEM.71.2.1084-1088.2005
67. Piñeiro C, Abuín JM, Pichel JC. 2020. Very fast tree: speeding up the estimation of phylogenies for large alignments through parallelization and vectorization strategies. Bioinformatics 36:4658–4659. https://doi.org/10.1093/bioinformatics/btaa582
68. Huang SQ, Zhang XY, Song ZW, Rahman MU, Fan B. 2023. Transcriptional profiling and transposon mutagenesis study of the endophyte *Pantoea eucalypti* FBS135 adapting to nitrogen starvation. Int J Mol Sci 24:14282. https://doi.org/10.3390/ijms241814282
69. Swamy CT, Gayathri D, Devaraja TN, Bandekar M, D'Souza SE, Meena RM, Ramaiah N. 2016. Plant growth promoting potential and phylogenetic characteristics of a lichenized nitrogen fixing bacterium, *Enterobacter cloacae*. J Basic Microbiol 56:1369–1379. https://doi.org/10.1002/jobm.201600197
70. Wang Z, Zhang H, Zhang D, Wang Y, Han Y, Xue X, Jiang Y. 2024. Biodegradation of phenol-contaminated soil and plant growth promotion by *Myroides xuanwuensis* H13. Microbiol Spectr 12. https://doi.org/10.1128/spectrum.00266-24:e0026624
71. Zhang TT, Hu F, Ma L. 2019. Phosphate-solubilizing bacteria from safflower rhizosphere and their effect on seedling growth. Open Life Sci 14:246–254. https://doi.org/10.1515/biol-2019-0028
72. Sun F, Ou Q, Wang N, Guo ZX, Ou Y, Li N, Peng C. 2020. Isolation and identification of potassium-solubilizing bacteria from *Mikania micrantha* rhizospheric soil and their effect on *M. micrantha* plants. Glob Ecol Conserv 23:e01141. https://doi.org/10.1016/j.gecco.2020.e01141
73. Mahdi I, Fahsi N, Hafidi M, Allaoui A, Biskri L. 2020. Plant growth enhancement using rhizospheric halotolerant phosphate solubilizing bacterium *Bacillus licheniformis QA1* and *Enterobacter asburiae QF11* isolated from *Chenopodium quinoa* willd. Microorganisms 8:948. https://doi.org/10.3390/microorganisms8060948
74. Shah S, Chand K, Rekadwad B, Shouche YS, Sharma J, Pant B. 2021. A prospectus of plant growth promoting endophytic bacterium from orchid (*Vanda cristata*). BMC Biotechnol 21:16. https://doi.org/10.1186/s12896-021-00676-9
75. Oliva G, Di Stasio L, Vigliotta G, Guarino F, Cicatelli A, Castiglione S. 2023. Exploring the potential of four novel halotolerant bacterial strains as plant-growth-promoting rhizobacteria (PGPR) under saline conditions. Appl Sci (Basel) 13:4320. https://doi.org/10.3390/app13074320
76. Hofmann M, Heine T, Malik L, Hofmann S, Joffroy K, Senges CHR, Bandow JE, Tischler D. 2021. Screening for microbial metal-chelating siderophores for the removal of metal ions from solutions. Microorganisms 9:111. https://doi.org/10.3390/microorganisms9010111
77. Liu X, Xu DQ, Wu DF, Xu MX, Wang Y, Wang WW, Ran TT. 2023. BarA/UvrY differentially regulates prodigiosin biosynthesis and swarming motility in *Serratia marcescens* FS14. Res Microbiol 174:104010. https://doi.org/10.1016/j.resmic.2022.104010
78. Lau T-TV, Puah S-M, Tan J-AMA, Merino S, Puthucheary SD, Chua K-H. 2023. Flagellar motility mediates biofilm formation in *Aeromonas dhakensis*. Microb Pathog 177:106059. https://doi.org/10.1016/j.micpath.2023.106059
79. Xing YH, Tan SX, Liu S, Xu SZ, Wan WJ, Huang QY, Chen WL. 2022. Effective immobilization of heavy metals via reactive barrier by rhizosphere bacteria and their biofilms. Environ Res 207:112080. https://doi.org/10.1016/j.envres.2021.112080
80. Kamnev AA, Dyatlova YA, Kenzhegulov OA, Fedonenko YP, Evstigneeva SS, Tugarova AV. 2023. Fourier transform infrared (FTIR) spectroscopic study of biofilms formed by the rhizobacterium *Azospirillum baldaniorum* Sp245: aspects of methodology and matrix composition. Molecules 28:1949. https://doi.org/10.3390/molecules28041949

81. Wang YY, Liu YD, Zheng KX, Xie LF, Ren Q, Yang ZH, Liao Q, Wang YL, Chen RH. 2021. The role of extracellular polymeric substances (EPS) in the reduction of Cr(VI) by *Pannonibacter phragmitetus* BB. J Environ Chem Eng 9:106163. https://doi.org/10.1016/j.jece.2021.106163
82. Shan LL, Bao XJ, Xu SY, Zhu ZB, Pei YY, Zheng WJ, Yuan YX. 2024. Biofilm formation and chlorine resistance of microbial communities in household drinking water system: Preliminary idea of using bacteria to control bacteria. Process Biochem 141:179–189. https://doi.org/10.1016/j.procbio.2024.04.004
83. Dehghanikhah F, Shakarami J, Asoodeh A. 2020. Purification and biochemical characterization of alkalophilic cellulase from the symbiotic *Bacillus subtilis* BC1 of the leopard moth, *Zeuzera pyrina* (L.) (Lepidoptera: Cossidae). Curr Microbiol 77:1254–1261. https://doi.org/10.1007/s00284-020-01938-z
84. Liu Y, Yao SX, Deng LL, Ming J, Zeng KF. 2019. Different mechanisms of action of isolated epiphytic yeasts against *Penicillium digitatum* and *Penicillium italicum* on citrus fruit. Postharvest Biol Technol 152:100–110. https://doi.org/10.1016/j.postharvbio.2019.03.002
85. Wu XR, Wang YX, Tong BD, Chen XH, Chen JH. 2018. Purification and biochemical characterization of a thermostable and acid-stable alpha-amylase from *Bacillus licheniformis* B4-423. Int J Biol Macromol 109:329–337. https://doi.org/10.1016/j.ijbiomac.2017.12.004
86. Medison RG, Jiang JW, Medison MB, Tan LT, Kayange CDM, Sun ZX, Zhou Y. 2023. Evaluating the potential of *Bacillus licheniformis* YZCUO202005 isolated from lichens in maize growth promotion and biocontrol. Heliyon 9:e20204. https://doi.org/10.1016/j.heliyon.2023.e20204
87. Chernyshov SV, Tsvetkova DV, Mikoulinskaia GV. 2023. A rapid and efficient technique for the isolation of *Bacillus* genomic DNA using A cocktail of peptidoglycan hydrolases of different type. World J Microbiol Biotechnol 39. https://doi.org/10.1007/s11274-022-03475-2
88. Chin C-S, Peluso P, Sedlazeck FJ, Nattestad M, Concepcion GT, Clum A, Dunn C, O'Malley R, Figueroa-Balderas R, Morales-Cruz A, Cramer GR, Delledonne M, Luo C, Ecker JR, Cantu D, Rank DR, Schatz MC. 2016. Phased diploid genome assembly with single-molecule real-time sequencing. Nat Methods 13:1050–1054. https://doi.org/10.1038/nmeth.4035
89. Chen S. 2023. Ultrafast one-pass FASTQ data preprocessing, quality control, and deduplication using fastp. Imeta 2:e107. https://doi.org/10.1002/imt2.107
90. Walker BJ, Abeel T, Shea T, Priest M, Abouelliel A, Sakthikumar S, Cuomo CA, Zeng QD, Wortman J, Young SK, Earl AM. 2014. Pilon: an integrated tool for comprehensive microbial variant detection and genome assembly improvement. PLoS One 9:e112963. https://doi.org/10.1371/journal.pone.0112963
91. Tatusova T, DiCuccio M, Badretdin A, Chetvernin V, Nawrocki EP, Zaslavsky L, Lomsadze A, Pruitt KD, Borodovsky M, Ostell J. 2016. NCBI prokaryotic genome annotation pipeline. Nucleic Acids Res 44:6614–6624. https://doi.org/10.1093/nar/gkw569
92. Lagesen K, Hallin P, Rodland EA, Staerfeldt H-H, Rognes T, Ussery DW. 2007. RNAmmer: consistent and rapid annotation of ribosomal RNA genes. Nucleic Acids Res 35:3100–3108. https://doi.org/10.1093/nar/gkm160
93. Chan PP, Lin BY, Mak AJ, Lowe TM. 2021. tRNAscan-SE 2.0: improved detection and functional classification of transfer RNA genes. Nucleic Acids Res 49:9077–9096. https://doi.org/10.1093/nar/gkab688
94. Nawrocki EP, Eddy SR. 2013. Infernal 1.1: 100-fold faster RNA homology searches. Bioinformatics 29:2933–2935. https://doi.org/10.1093/bioinformatics/btt509
95. Stothard P, Wishart DS. 2005. Circular genome visualization and exploration using CGView. Bioinformatics 21:537–539. https://doi.org/10.1093/bioinformatics/bti054
96. Jain C, Rodriguez-R LM, Phillippy AM, Konstantinidis KT, Aluru S. 2018. High throughput ANI analysis of 90K prokaryotic genomes reveals clear species boundaries. Nat Commun 9:5114. https://doi.org/10.1038/s41467-018-07641-9
97. Carroll LM, Wiedmann M, Kovac J. 2020. Proposal of a taxonomic nomenclature for the *Bacillus cereus* group which reconciles genomic definitions of bacterial species with clinical and industrial phenotypes. mBio 11:e00034-20. https://doi.org/10.1128/mBio.00034-20
98. Xu S, Li L, Luo X, Chen M, Tang W, Zhan L, Dai Z, Lam TT, Guan Y, Yu G. 2022. Ggtree: a serialized data object for visualization of a phylogenetic tree and annotation data. Imeta 1:e56. https://doi.org/10.1002/imt2.56
99. Chen CJ, Wu Y, Li JW, Wang X, Zeng ZH, Xu J, Liu YL, Feng JT, Chen H, He YH, Xia R. 2023. TBtools-II: a "one for all, all for one" bioinformatics platform for biological big-data mining. Mol Plant 16:1733–1742. https://doi.org/10.1016/j.molp.2023.09.010
100. Fischer S, Brunk BP, Chen F, Gao X, Harb OS, Iodice JB, Shanmugam D, Roos DS, Stoeckert CJ. 2011. Using OrthoMCL to assign proteins to OrthoMCL - DB groups or to cluster proteomes into new ortholog groups. CP Bioinformatics 35. https://doi.org/10.1002/0471250953.bi0612s35
101. Darling ACE, Mau B, Blattner FR, Perna NT. 2004. Mauve: multiple alignment of conserved genomic sequence with rearrangements. Genome Res 14:1394–1403. https://doi.org/10.1101/gr.2289704
102. Zheng JF, Ge QW, Yan YC, Zhang XP, Huang L, Yin YB. 2023. dbCAN3: automated carbohydrate-active enzyme and substrate annotation. Nucleic Acids Res 51:W115–W121. https://doi.org/10.1093/nar/gkad328